



OPEN ACCESS

EDITED BY

Shuting Liu,
Kean University, United States

REVIEWED BY

Luis Manuel Bolaños,
University of Exeter, United Kingdom
Andrew Decker Steen,
The University of Tennessee, Knoxville,
United States

*CORRESPONDENCE

You-Shao Wang
✉ yswang@scsio.ac.cn

RECEIVED 06 March 2023

ACCEPTED 31 May 2023

PUBLISHED 21 June 2023

CITATION

Sun C-C, Zhao W-J, Yue W-Z, Cheng H, Sun F-L, Wang Y-T, Wu M-L, Engel A and Wang Y-S (2023) Polymeric carbohydrates utilization separates microbiomes into niches: insights into the diversity of microbial carbohydrate-active enzymes in the inner shelf of the Pearl River Estuary, China.
Front. Microbiol. 14:1180321.
doi: 10.3389/fmicb.2023.1180321

COPYRIGHT

© 2023 Sun, Zhao, Yue, Cheng, Sun, Wang, Wu, Engel and Wang. This is an open-access article distributed under the terms of the [Creative Commons Attribution License \(CC BY\)](https://creativecommons.org/licenses/by/4.0/). The use, distribution or reproduction in other forums is permitted, provided the original author(s) and the copyright owner(s) are credited and that the original publication in this journal is cited, in accordance with accepted academic practice. No use, distribution or reproduction is permitted which does not comply with these terms.

Polymeric carbohydrates utilization separates microbiomes into niches: insights into the diversity of microbial carbohydrate-active enzymes in the inner shelf of the Pearl River Estuary, China

Cui-Ci Sun^{1,2}, Wen-Jie Zhao^{1,3}, Wei-Zhong Yue¹, Hao Cheng¹, Fu-Lin Sun^{1,2}, Yu-Tu Wang², Mei-Lin Wu¹, Anja Engel⁴ and You-Shao Wang^{1,2*}

¹State Key Laboratory of Tropical Oceanography, South China Sea Institute of Oceanology, Chinese Academy of Sciences, Guangzhou, China, ²Daya Bay Marine Biology Research Station, Chinese Academy of Sciences, Shenzhen, China, ³University of Chinese Academy of Sciences, Beijing, China, ⁴GEOMAR Helmholtz Centre for Ocean Research Kiel, Kiel, Germany

Polymeric carbohydrates are abundant and their recycling by microbes is a key process of the ocean carbon cycle. A deeper analysis of carbohydrate-active enzymes (CAZymes) can offer a window into the mechanisms of microbial communities to degrade carbohydrates in the ocean. In this study, metagenomic genes encoding microbial CAZymes and sugar transporter systems were predicted to assess the microbial glycan niches and functional potentials of glycan utilization in the inner shelf of the Pearl River Estuary (PRE). The CAZymes gene compositions were significantly different between in free-living (0.2–3 μm, FL) and particle-associated (>3 μm, PA) bacteria of the water column and between water and surface sediments, reflecting glycan niche separation on size fraction and selective degradation in depth. Proteobacteria and Bacteroidota had the highest abundance and glycan niche width of CAZymes genes, respectively. At the genus level, *Alteromonas* (Gammaproteobacteria) exhibited the greatest abundance and glycan niche width of CAZymes genes and were marked by a high abundance of periplasmic transporter protein TonB and members of the major facilitator superfamily (MFS). The increasing contribution of genes encoding CAZymes and transporters for *Alteromonas* in bottom water contrasted to surface water and their metabolism are tightly related with particulate carbohydrates (pectin, alginate, starch, lignin-cellulose, chitin, and peptidoglycan) rather than on the utilization of ambient-water DOC. *Candidatus Pelagibacter* (Alphaproteobacteria) had a narrow glycan niche and was primarily preferred for nitrogen-containing carbohydrates, while their abundant sugar ABC (ATP binding cassette) transporter supported the scavenging mode for carbohydrate assimilation. Planctomycetota, Verrucomicrobiota, and Bacteroidota had similar potential glycan niches in the consumption of the main component of transparent exopolymer particles (sulfated fucose and rhamnose containing polysaccharide and sulfated-N-glycan), developing considerable niche overlap among these taxa. The most abundant CAZymes and transporter genes as well as the widest glycan niche in the abundant bacterial taxa implied their potential key roles on the organic carbon utilization, and the high degree of glycan niches separation and polysaccharide

composition importantly influenced bacterial communities in the coastal waters of PRE. These findings expand the current understanding of the organic carbon biotransformation, underlying the size-fractionated glycan niche separation near the estuarine system.

KEYWORDS

microbial CAZyme diversity, metagenomics analysis, glycan niche, the Pearl River Estuary, microbiome

1. Introduction

Carbohydrates constitute a large fraction of labile and semi-labile organic matter and mainly derive from phytoplankton in the ocean (Pakulski and Benner, 1994). Much of the total carbohydrate fraction is combined in oligo- and polysaccharides (Benner, 2002; Mykkestad and Børsheim, 2007; Sperling et al., 2017), and polysaccharides (i.e., glycans) can contribute up to 50% to total phytoplankton biomass (Painter, 1983; Becker et al., 2020). Carbohydrate degradation in the ocean is mainly driven by prokaryotic organisms. Labile polysaccharides are rapidly degraded and respired. Polysaccharides in sinking particles are remineralized while sinking through the water column or in sediments where the more recalcitrant fraction may accumulate (Jiao et al., 2011; Arnosti et al., 2021). Thus, particulate polysaccharides can contribute substantially to carbon export from surface waters (Vidal-Melgosa et al., 2021).

Polysaccharides are chemically diverse and contain various structures and highly branched molecules. CAZymes are used by heterotrophic microbes to assemble, break down, and modify glycans and glycoconjugates. In general, the diversity of CAZymes can mirror the substrates that they utilize and the ecological and/or biogeochemical processes in the ocean (Teeling et al., 2012, 2016; Zhao et al., 2020; Baltar et al., 2021). In addition, long-term investigations carried out by Teeling et al. (2016) revealed that variations of CAZymes genes traits and the accompanying succession of bacterial compositions are largely governed by deterministic principles such as substrate-induced forcing. Furthermore, Vidal-Melgosa et al. (2021) found that the abundance of CAZymes in the North Sea of the Atlantic Ocean involved in the degradation of laminarin was much higher than fucoidan during the outbreak of diatom bloom, resulting in the carbon sequestration in the form of fucoidan (Vidal-Melgosa et al., 2021). For alginate and pectin, identified alginate-degrading enzymes and polysaccharide utilization loci (PULs) in metagenome-assembled genomes related to Alteromonadacea and Bacteroidetes in seawater indicated that these CAZyme gene pools are not phylogenetically widespread but niche specialized (Hehemann et al., 2017; Thomas et al., 2021; Wolter et al., 2021). Bacteroidota, Planctomycetota, and Verrucomicrobiota phylum are prominent for the degradation of a wide range of complex carbohydrates (i.e., plant cell wall, bacterial EPS, and sulfated glycan) due to their high diversity of CAZymes and sulfatases, which improve their adaptability in many diverse environments (Costa et al., 2020; Sichert et al., 2020; Luis et al., 2022).

Niche is a complex description of how a microbial species uses its environment. For a long time, less attention has been paid to the

ecological niche concept of microbiome than to other plants and animals. Microbial niche breadth has been measured for specific aspects of the environment [e.g., temperature (Sauer et al., 2015), pH (Kuang et al., 2013)] and nutrient availability (Kits et al., 2017; Herold et al., 2020; Dal Bello et al., 2021). Recently, von Meijenfildt et al. (2023) used social niche breadth score to reveal niche range strategies of generalists and specialists, based on the variability of the communities with which it associates. Since metabolic traits (such as the ability to metabolize certain substrates or synthesize molecules) are the most important factors affecting the niche of microbial cells (Garza et al., 2018; Fahimipour and Gross, 2020; Dal Bello et al., 2021), and the polymers of carbohydrates represent a large pool of organic matter in the ocean, CAZymes diversity, glycan niche width and the related measurement of glycan overlap based on the CAZymes genes distribution in the microbial community are presumably closely related to microbial utilization of the organic carbon matter in the environment and their niche specifications (Teeling et al., 2012, 2016; Smits et al., 2017; Avci et al., 2020; Dal Bello et al., 2021).

Besides CAZymes, outer membrane transporters specific for polysaccharide uptake, such as the SusC-like TonB-dependent transporter (TBDT) (starch utilization system), also can serve as an indicator for estimating bacterial polysaccharide utilization (Francis et al., 2021). Recently, according to a new model of the strategy of microbial processing polysaccharides degradation production, marine microbes were simplified into three types: sharer, scavenger, and selfish bacteria (Reintjes et al., 2019). Sharers are bacteria that secrete extracellular enzymes and hydrolyze substrates in the external environment; oppositely, scavengers cannot produce corresponding enzymes for high molecular weight polysaccharides and are considered to benefit from hydrolysis products (e.g., oligosaccharide) degraded by sharers. The selfish bacteria are defined as hydrolyzing substrates with little diffusive loss (Reintjes et al., 2019; Arnosti et al., 2021). In general, the selfish bacteria have abundant cell-associated enzymes and transporters in outer membranes (e.g., SusC), which enable the hydrolysates quickly come into the periplasm space instead of being utilized by other bacteria (Cuskin et al., 2015). The insights from bacterial CAZymes diversity contribute to the understanding of algae-bacteria interactions and the remineralization of polysaccharides in the light of large amounts of algae primary productivity on global scales. So far, polysaccharide-degrading capabilities of marine bacteria *in situ* driven by CAZymes are largely unknown (Lazar et al., 2016; Orsi et al., 2018).

Estuaries and adjacent waters with enhanced nutrient concentrations are typically highly productive and show elevated polysaccharide concentrations including algal storage polysaccharides

(β -1,3-glucans such as laminarin; α -1,4-glucans such as starch and glycogen) (Alderkamp et al., 2007), and cell matrix and cell wall constituents of both algae and other organisms (cellulose or hemicellulose, xylose, lignin, peptidoglycan, pectin, and chitin) (Okuda, 2002; Tremblay and Benner, 2006). Moreover, transparent exopolymer particles (TEP) are ubiquitous in estuarine systems. These gel-like particles are rich in acidic polysaccharides, which include fucose- and rhamnose-rich sulfated heteropolysaccharides (sulfate half-ester) or uronic acid-containing polysaccharides with carboxyl groups, such as alginate and pectin (Hung et al., 2001; Passow, 2002; Sperling et al., 2017). In addition, terrestrial higher plants are rich in lignin and cellulose and are often exported to estuaries and adjacent coastal seas (Benner and Kaiser, 2011). In the transition zone from the estuary and shelf to the continent, carbohydrates undergo significant degradation and transformation processes (Benner, 2004). Accordingly, bacterial CAZymes perform complex functions and are responsible for much of the carbon turnover in the estuary, characterized by high loads of organic carbon. Yet, little is known about the diversity of microbial CAZymes and their role in polysaccharide decomposition in the estuarine system (Baker et al., 2015; Smith et al., 2019).

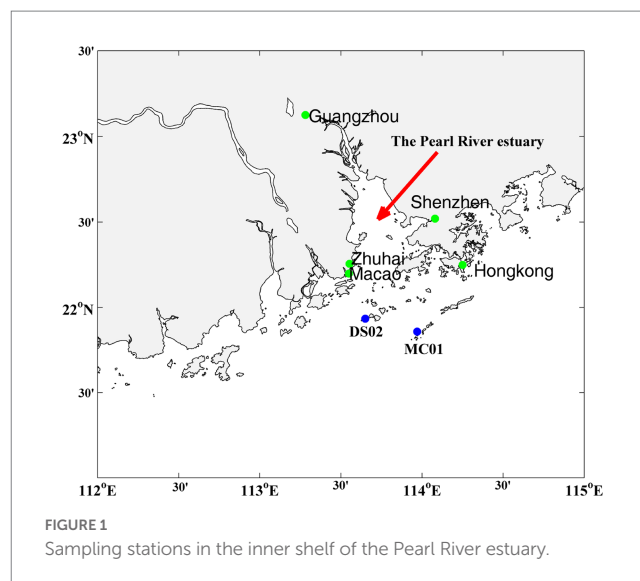
In this study, we sampled the inner shelf of the Pearl River Estuary, where the contribution of terrigenous organic carbon was on average $34 \pm 4\%$ while polysaccharides and proteinaceous matter were mainly derived from phyto- and bacterioplankton (He et al., 2010a,b; Zhang and Ran, 2014; Sun et al., 2022). In addition, TEP was an important particulate component of the total organic pool in the PRE (Sun et al., 2012). A recent study found that the particle-associated bacteria communities in the PRE differed from free-living bacteria compositions (Liu Y. Y. et al., 2020) and showed higher connectivity between bacterioplankton and archaea plankton communities than free-living bacteria (Wang et al., 2020).

To reveal the microbial consortia involved in the transformation of functionally different polysaccharides, genes of microbial CAZymes, sugar transporter, sulfatase, and their functional potentials of polysaccharide utilization were predicted for different size fractions, representing free-living bacteria ($0.2\text{--}3\ \mu\text{m}$) and particle-associated bacteria ($>3\ \mu\text{m}$) in water and surface sediments of the inner PRE based on metagenomic data. We assessed microbial CAZymes diversity, glycan niche width, glycan specificities, and metabolic strategies for implying organic carbon turnover in the inner shelf of the estuarine system.

2. Sampling and method

2.1. Sampling

The study was conducted on the inner shelf of the PRE in Nov 2020. The sampling sites are shown in Figure 1. Water samples were collected near the surface (0.5 m depth) and bottom layers, using 5.0-L Niskin bottles. 2 L of seawater was filtered first through $3\text{-}\mu\text{m}$ -pore-size and subsequently through $0.22\text{-}\mu\text{m}$ -pore-size filter membranes (Millipore, Bedford, United States) to collect particle-associated ($>3\ \mu\text{m}$) and free-living bacteria ($0.2\text{--}3\ \mu\text{m}$), respectively. The surface sediment (upper 1–2 cm) was collected using a grab sampler. The filter membranes and surface sediment (15 g) were frozen immediately in liquid nitrogen before being stored at -80°C until DNA extraction.



Salinity, pH, turbidity, and temperature were measured *in situ* using a YSI 6600 probe (YSI Inc., United States).

2.2. Chemical analysis

For particulate organic carbon (POC) and Chl_a, 1 L of seawater was filtered through pre-combusted (10 h, 450°C) glass fiber filters ($0.7\ \mu\text{m}$ pore size, Whatman, USA) under a gentle vacuum of $<150\ \text{mm Hg}$. From each sample, 30 mL of filtrate was collected into 40 mL pre-combusted glass vials and immediately stored at -20°C for dissolved organic carbon (DOC) analysis. 200 mL of filtered seawater from each depth were stored at -20°C for nutrient analysis (nitrate, nitrite, ammonium salt, phosphate, and silicate). Chl_a concentrations were determined after extraction in 90% acetone overnight (Parsons et al., 1984). The concentration of POC was determined with a PE2400 Series II CHNS/O analyzer (PerkinElmer, USA). DOC concentration was measured using a Shimadzu TOC-V analyzer (Shimadzu Inc., Japan) (Sun et al., 2012). Nutrients were determined using a four-channel continuous flow Technicon AA3 auto-analyzer (Bran+Luebbe GmbH, Germany), and the detection limits were about $0.04\ \mu\text{mol L}^{-1}$ for inorganic nitrogen nutrients and $0.03\ \mu\text{mol L}^{-1}$ for phosphate and silicate, respectively.

For TOC in sediment, samples were oven-dried at 50°C , ground, and homogenized with a pestle and mortar, then passed through a mesh sieve ($250\ \mu\text{m}$ in pore size). Sediment samples were soaked in $1\ \text{mol L}^{-1}$ HCl at room temperature for 24 h (Prahl et al., 1994), rinsed with Milli-Q water to remove salts, and then oven-dried at 50°C . Then, TOC was detected using dry combustion with a Perkin-Elmer 2400 CHNS/O analyzer. The relative standard deviations (RSDs) of TOC determinations were $<5\%$. The content of Acid Volatile Sulfide (AVS) in sediments was measured with the methylene-blue-spectrophotometric method according to the standard method of the People's Republic of China (HJ 833-2017). Then, 3.0 g of wet sample was put into the nitrogen-purging meter (Taipute Co. Ltd., LHW-6A) at first, and (1 + 2) HCl was dripped in. H_2S produced in the nitrogen-purging meter was absorbed by the mixed solution of zinc acetate and sodium acetate. Finally, the content of AVS in the mixed solution was measured with the UV spectrophotometer (Shimadzu, UV-1700).

2.3. DNA preparation, sequencing, metagenome assembly, and analysis

Sample DNA was extracted in triplicate from 0.5 g of fresh surface sediment and filtered samples using the Fast DNA spin kit (MP Biomedicals, Cleveland, United States) following the manufacturer's instructions. The quality and integrity of the DNA extracts were assessed using a NanoDrop 2000 spectrophotometer. The extracted microbial DNA was processed to construct metagenome shotgun sequencing libraries with insert sizes of 350 bp using the Illumina TruSeq Nano DNA LT Library Preparation Kit. Each library was sequenced by an Illumina HiSeq X-ten platform (2 × 150; Illumina, USA) at Nuohe Biotechnology Co., Ltd. (Tianjin, China). The sequences can be found on the National Center for Biotechnology Information (NCBI), with the accession number PRJNA859198.

Metagenomic raw reads were quality-checked with FASTQC v0.11.8 (Davis et al., 2013) and the evaluation of clean reads quality was trimmed with a sliding window approach using Trimmomatic (Bolger et al., 2014). Trimmed reads were processed and assembled using MEGAHIT with default settings (Bankevich et al., 2012); Open reading frames (ORFs) were identified by the Prodigal software (Hyatt et al., 2010) and further annotated for function and taxa identification (Buchfink et al., 2015). Filtered reads were mapped to the ORFs using Bowtie2 to calculate the abundance of each ORF (Langmead and Salzberg, 2012). Taxonomic classifications of the metagenomic sequencing reads from each sample were performed against the NR database (non-redundant proteins database, downloaded from <ftp://ftp.ncbi.nlm.nih.gov/blast/db>), which included proteins from archaea, bacteria, viruses, and fungi.

Annotation of CAZymes was done using dbCAN v10 against the CAZy database v09242021 based on hmmer filter (Zhang et al., 2018) and additionally confirmed using DIAMOND BLAST (Buchfink et al., 2015), and CAZymes were only analyzed for contigs >500 bp. Sulfatases were predicted with Blast v2.10.1 against the SulfAtlas database Version 2.3.1 (Barbeyron et al., 2016).¹ Reads per kilobase per million (RPKM = 1,000,000 × (number of reads mapped/gene length in kilobase pairs)/number of reads in sample) values were calculated to estimate the normalized relative abundance of individual gene families. The phylogenetic affiliation of CAZyme was determined using the lowest common ancestor algorithm adapted from the DIAMOND blast by searching against the nonredundant database (Buchfink et al., 2015; Zhao et al., 2020). There was no bias toward better predictions in individual taxonomic groups based on the CAZy database. However, the possibility of a systematic under-sampling of CAZyme diversity for individual clades cannot be excluded. The functional potentials annotations at the CAZyme family level were further grouped and assigned to substrate targets according to the common designations from the CAZyme database.² Annotation of carbohydrate transporters was done using Kofam KOALA v1.3.0 against the KEGG database³ with the e-value cutoff of 10⁻⁵ (Aramaki et al., 2020), and additionally checked by TCDB database (The Transporter Classification Database) (Saier et al., 2021).⁴ We used

SignalP 6.0 (Teufel et al., 2022) and Deep TMHMM (Hallgren et al., 2022) to predict the secreted CAZymes and subcellular localization.

2.4. Glycan niches measures

CAZymes microbial diversity and glycan niche width were indicated by the Shannon index and Levins index, respectively (Peterson et al., 2011; Baltar et al., 2021). This article focused on the degradation of carbohydrates; therefore, glycan niches measures and all analyses in the results section were based on the degradative CAZymes classes (Aas, Ces, CBMs, PLs, and GHs) excluding GTs.

Levins index can be calculated using the following equations:

$$B = \frac{1}{\sum p_j^2}$$

Where B is glycan niche width indicated by Levins index, j refers to individual CAZyme family genes, p_j is the proportion of j abundance in the total CAZymes gene abundance of the taxa. To standardize Levins niche width to a scale of 0–1, we use the equation:

$$B_A = \frac{B-1}{n-1}$$

Where B_A is the standardized Levins niche width, n is the total number of CAZymes families predicted in metagenomic fragments.

The Shannon-Wiener index was calculated by the following equation:

$$B_i = -\sum_{j=1}^n (p_{i,j} \ln p_{i,j})$$

Where B_i is the Shannon-Wiener index of CAZyme gene abundance evenness for bacterial taxon i ; j refers to individual CAZyme family genes, n is the total numbers of CAZymes families in taxa i , $n_{i,j}$ is the CAZymes family gene j abundance of the bacteria taxa i , N_i is the abundance of CAZyme genes in bacterial taxon i excluding GTs, $p_{i,j}$ is the proportion of CAZymes family gene j abundance to N_i of the bacteria taxa i ($j = 1, 2, 3, 4, \dots, n$).

The overlapping index of glycan niche between taxa i and k ($O_{i,k}$) was calculated using the Morisita-Horn index by the following equations (Peterson et al., 2011):

$$O_{i,k} = \frac{2\sum_i^n p_{i,j} p_{i,k}}{\sum_i^n p_{i,j}^2 + \sum_i^n p_{i,k}^2}$$

Where $p_{i,j}$ is the proportion of CAZymes i in the total CAZymes abundance in taxa j ; $p_{i,k}$ is the proportion CAZymes i in the total CAZymes abundance in taxa k ; n is the total number of CAZymes families (i is 1, 2, 3, ... n).

2.5. Statistical analysis

Principal Co-ordinates Analysis (PCoA) of metagenomic CAZymes data was done between free-living and particle-associated

1 <http://abims.sb-roscoff.fr/sulfatlas/index.html>

2 www.cazy.org

3 <https://www.genome.jp/kegg/>

4 <https://tcdb.org/>

fractions in water and between the water column and sediment samples using Permutational Multivariate Analysis of Variance (PerMANOVA) (999 permutations) using the R package *vegan* (Oksanen et al., 2022). STAMP (Statistical Analysis of Metagenomic Profiles) was used to search for CAZymes families differences across the different groups between surface and bottom water and between free-living and particle-associated fractions (Parks and Beiko, 2015). Nonparametric statistics (Wilcoxon–Mann–Whitney test) were done to compare differences between the metagenomic data, and statistical significance was accepted for $p < 0.05$. Average values are given by the statistical mean and its standard deviation (SD). Spaa (Zhang and Ma, 2013) and ggplot2 (Ginestet, 2011) were used for ordination, diversity and niche calculation, and visualization, respectively.

3. Results

3.1. Environmental parameters and microbial composition

Environmental data for water and surface sediment in the inner shelf of the PRE are given in [Supplementary Tables S1, S2](#). Salinity was over 32 throughout the water column, indicating the strong influence of offshore oceanic water in winter. The total dissolved inorganic nitrogen and phosphate concentrations were lower than 10 and $0.2 \mu\text{molL}^{-1}$, respectively, yielding N/P far above the Redfield ratio (16:1), thus indicating potential phosphate limitation in the study region. Phosphate deficiency likely reduced *Chla* concentration ($0.74\text{--}1.53 \mu\text{gL}^{-1}$). These results indicate relative nutrient-poor status during the sampling time. The concentration of acid-volatile sulfide was seven times higher at St DS02 than at St MC01, likely related to the pollution by aquaculture since DS02 was close to artificial reefs around Wan shan Island.

The proportions of bacteria in the total microbial sequences were 72–82% and 84.6–86% in water and sediment, respectively ([Supplementary Table S4](#)). Bacterial communities showed significant differences between water and sediment ([Figure 2A](#)). Alphaproteobacteria (17.99–33.63%), Gammaproteobacteria (14.18–24.82%), Bacteroidota (6.59–8.06%), Actinomycetota (3.86–7.51%) and Verrucomicrobiota (1.27–1.94%) were the most abundant phyla in the water. In the sediments, however, the contributions of Alphaproteobacteria, Gammaproteobacteria, Bacteroidota, Actinomycetota, and Verrucomicrobiota were reduced, and Deltaproteobacteria (25.71–26.26%) were the most abundant. In addition, contributions of Chloroflexota (5.90–6.15%) and Nitrospirota (3.55–4.12%) in sediments were significantly higher than those in the water column in this study. At the genus level, the most abundant bacterial genera in this study were *Candidatus Pelagibacter* (7.33–14.89%), *Alteromonas* (0.52–12.95%) in water, and *Woeseia* (3.56–3.64%) in sediment, respectively ([Figure 2B](#)). A high proportion of *Alteromonas* in the bottom water particle samples (8.85–12.94%) was observed compared to all the surface water samples (0.52–2.71%).

3.2. Vertical and size-fractionated distributions of CAZymes families genes

The most abundant enzyme class genes were glycosyltransferases (GTs) ([Supplementary Figure S1](#)), followed by glycoside hydrolases (GHs). CEs (carbohydrate esterases), AAs

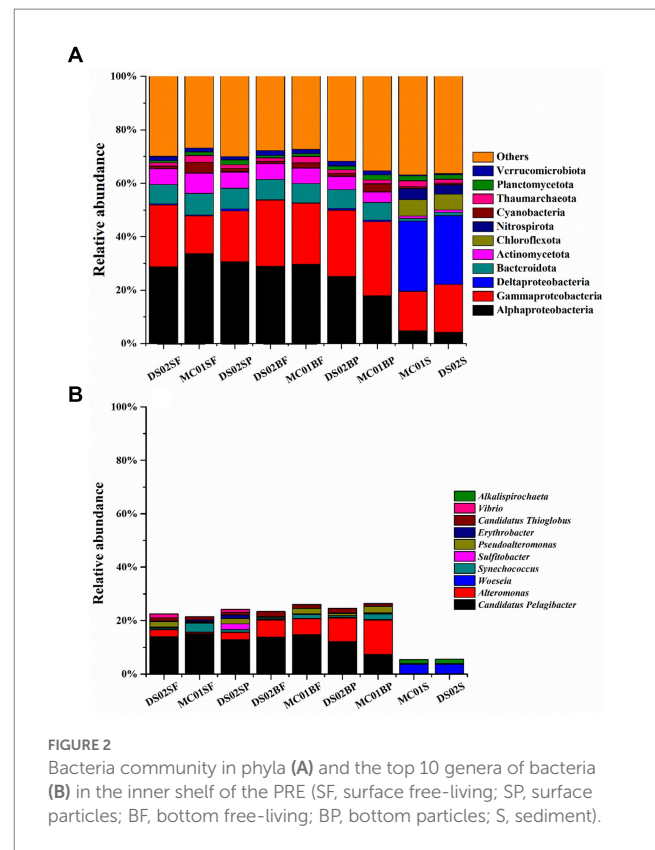
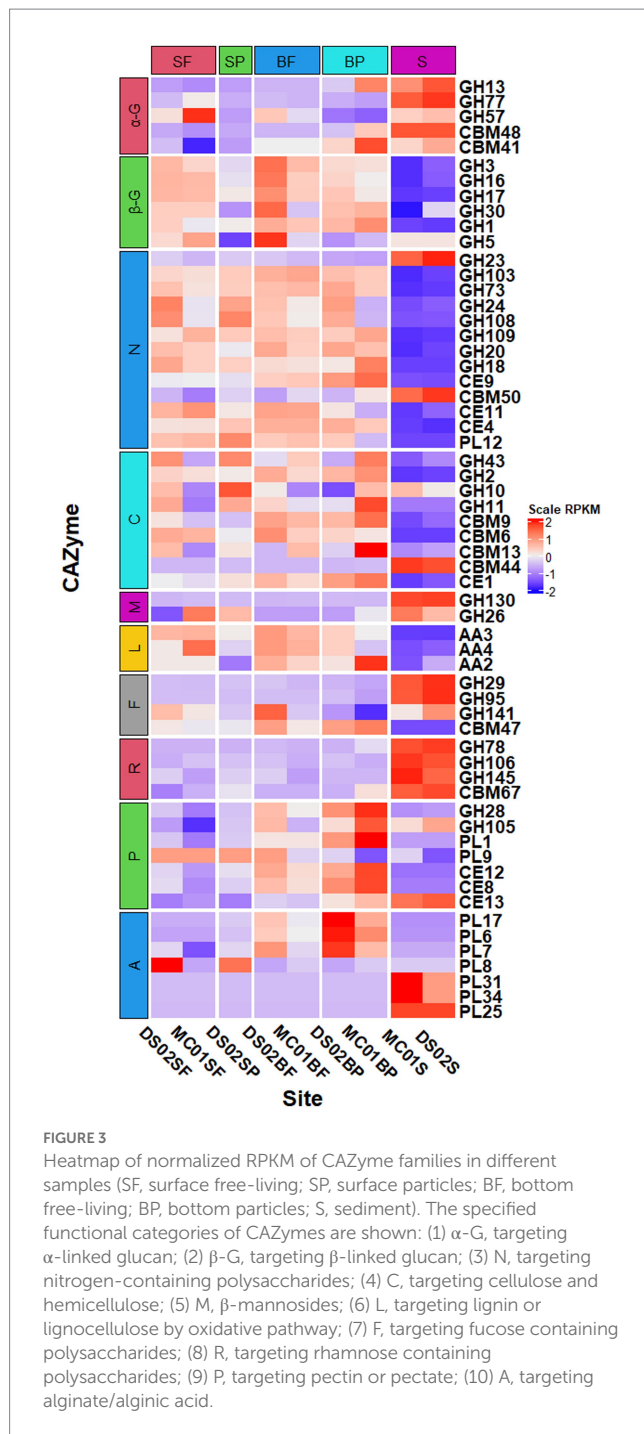


FIGURE 2

Bacteria community in phyla (A) and the top 10 genera of bacteria (B) in the inner shelf of the PRE (SF, surface free-living; SP, surface particles; BF, bottom free-living; BP, bottom particles; S, sediment).

(auxiliary activities associated with polysaccharide and lignin degradation), CBMs (carbohydrate-binding modules), and PLs (polysaccharide lyases). The relative abundance of genes encoding CAZymes classes differed significantly between water and sediment ([Supplementary Figure S1](#)), i.e., AAs, CEs, and PLs classes were significantly more abundant in the water samples ($p < 0.05$). This article focused on the degradation of carbohydrates, therefore, this study showed the annotation results on the degradative CAZymes genes except for GTs in the following sections. The CAZymes gene frequency of Σ (GHs + CBMs + CEs + PLs) was 0.55% in water and 0.36% in sediment, respectively ([Supplementary Table S5](#)). In this study, a total of 279 CAZymes families were identified, including 119 GHs and 79 GTs, 35 CBMs, 23 PLs, 13 CEs, and 10 AAs ([Supplementary Table S6](#), the top GH, CE, AA, PL, and CBM families were shown in [Supplementary Figures S2–S4](#), and their main functions were listed in [Supplementary Table S7](#)).

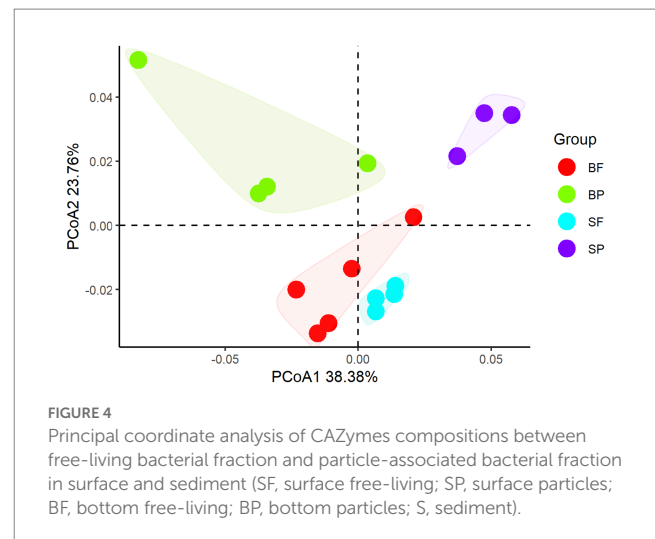
Principal coordinate analysis of CAZymes genes ([Figure 3](#)) and heat maps ([Figure 4](#)) indicate the presence of different CAZymes gene compositions between free-living bacterial fraction and particle-associated bacterial fraction (PERMANOVA, $R^2 = 0.59$, $p < 0.05$) ([Figure 3](#)) and between water and sediment (PERMANOVA, $R^2 = 0.20$, $p < 0.001$). The FL fraction has more abundant genes encoding AA3, 4, 6 (for lignin-cellulose), GH16, GH17, GH30 in surface (laminarinase), GH3 and GH5 (β -glucanase or glucosidase for oligo β -glucan), GH31, GH57, GH4, CBM6, CE3, CE11 than PA (Wilcoxon–Mann–Whitney test, $p < 0.05$) ([Supplementary Figures S2, S3](#)). In addition, the relative abundance of PLs genes was significantly higher in the particle-associated fraction of bottom waters (Wilcoxon–Mann–Whitney test, $p < 0.05$), such as PL1, 6, 7, and 17 ([Figure 4](#)). It reflected that the spectrum of PL genes was wider in the bottom particles and carboxyl acid polysaccharides were undergone deeply degraded by bacteria in the



bottom water. The relative gene abundance of CBM48, 50, 67, and 44 was higher in sediment than in water (Wilcoxon–Mann–Whitney test, $p < 0.05$) (Supplementary Figure S3), and associated with a higher abundance of their binding GHs genes in sediment, such as GH13, 77, and 31 targeting α-glucan, GH23 targeting peptidoglycan and GH78 (rhamnosidases).

3.3. Five classes of CAZymes distributions in bacterial communities

Regarding the contributions of bacterial taxa to the total CAZymes genes, a similar distribution was observed compared with



the bacteria composition at the phylum level (Figure 5A). At the genus level, for *Alteromonas* and *Candidatus Pelagibacter*, their contributions to the total CAZymes genes abundance ranged from 1.1–25.5% and 10.5–23.7% in water (Figure 5B), respectively. Figure 6A shows the counts of the number and relative abundance of GHs, PLs, CEs, AAs, and CBMs genes at the genus level. For GHs, the top contribution genera for GHs were i) *Alteromonas*, *Pseudoalteromonas*, *Vibrio*, *Candidatus Thioglobus*, *Aestuariibacter*, *Marinomonas* (Gammaproteobacteria), ii) *Candidatus Pelagibacter*, *Erythrobacter*, and *Ruegeria* (Alphaproteobacteria), iii) *Polaribacter* and *Formosa* (Bacteroidota), and iv) *Rhodopirellula* (Planctomycetota genus) (Figure 6A). PLs gene distribution in bacteria was similar to GHs, in which genus *Alteromonas* had the highest abundance and number of PLs genes in water. *Candidatus Pelagibacter* were the most prominent in CEs and AAs genes in water (Figure 6A). In addition, AAs genes were characterized by high abundance in Roseobacter Clade (*Sulfitobacter*, *Roseovarius*, *Ruegeria*, *Marinovum*, *Planctomarina*) belonging to Alphaproteobacteria. AAs are fundamental to facilitating lignin oxidation, even though they can not degrade lignin directly. Therefore, the wide distribution of genes encoding AAs in Alphaproteobacteria indicated that they were primary candidates to assist lignin-modifying enzymes for lignin degradation in this region. Unlike the distribution of CEs and AAs, no CBMs family genes were detected in *Candidatus Pelagibacter*, although they contained abundant CAZymes genes (Figure 6A). In contrast, besides *Pseudoalteromonas*, *Vibrio*, *Alteromonas* (Gammaproteobacteria) and *Polaribacter* (Bacteroidota), *Rhodopirellula*, *Mariniblastus*, *Blastopirellula*, *Planctomyces*, *Schlesneria*, *Gemmata* (Planctomycetota) and *Pedosphaera*, *Roseibacillus*, *Prosthecoibacter* (Verrucomicrobiota) were rich in CBMs genes in water, suggesting these communities were specialists for complex polysaccharide degradation.

In this study, *Woeseia* (Gammaproteobacteria) was the dominant genus in sediment concerning the relative abundance of CAZymes genes (Figure 6B). However, regarding the numbers of CAZymes families, *Sphingomonas* (Alphaproteobacteria), *Gemmatimonas* (Gemmatimonadetes), *Colwellia* and *Halioglobus* (Gammaproteobacteria), *Rhodopirellula* and *Blastopirellula* (Planctomycetota) showed a high diversity of CAZymes in sediment (Figure 6B).

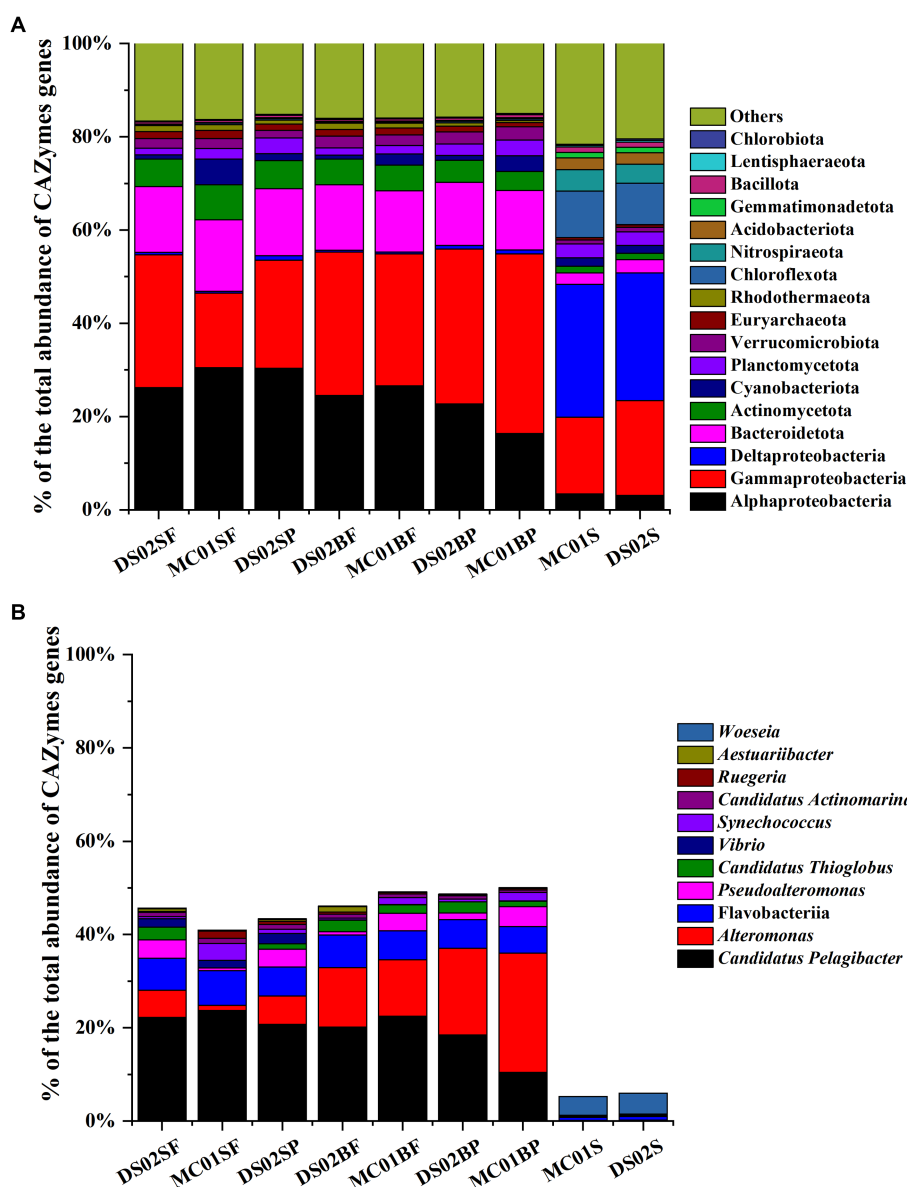


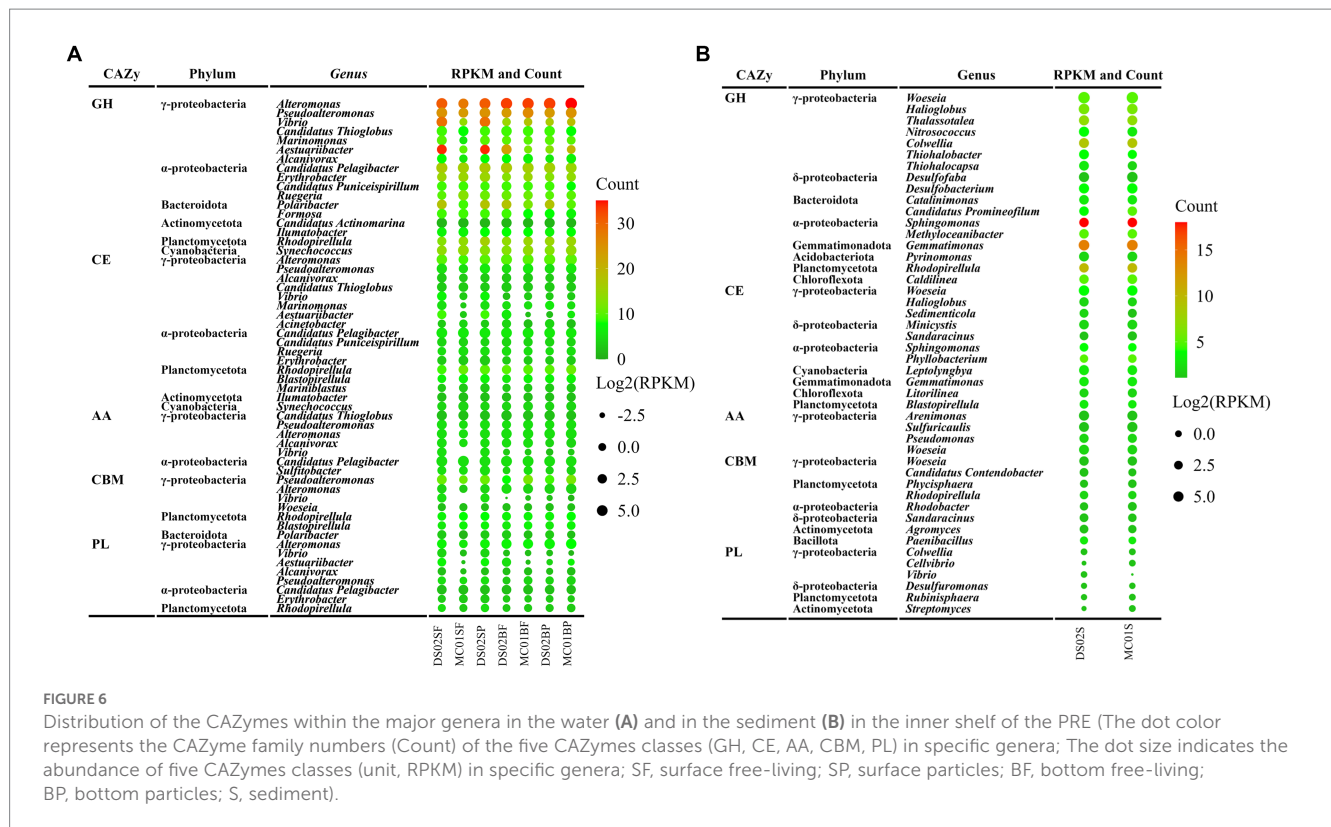
FIGURE 5 Contributions of the dominant taxa to the total CAZymes abundance (A: phylum; B: genus and class; SF, surface free-living; SP, surface particles; BF, bottom free-living; BP, bottom particles; S, sediment).

3.4. The glycan niche index in bacterial communities

In water, the Levins index and Shannon index generally showed a similar pattern of diversity of CAZymes families at the phylum level (Figure 7). The highest Shannon diversity index was found in Bacteroidota (3.64), Gammaproteobacteria (3.63), Planctomycetota (3.31), and Verrucomicrobiota (3.32) (Figure 7) in water, while in the sediment the index from high to low was found in Planctomycetota (3.43), Bacteroidota (3.43), Alphaproteobacteria (3.36), Gammaproteobacteria (3.27), and Chloroflexota (3.16), suggesting these communities had potentially wide glycan niches (Figure 7). At the genus level, the highest Levins index and Shannon index were observed in *Alteromonas* and *Pseudoalteromonas* in water

and *Sphingomonas* in sediment, respectively (Supplementary Figure S5).

Taxa with a wider niche width usually have higher metabolic flexibility, thus being less affected by environmental fluctuations, whereas rare taxa were more easily influenced by environmental disturbances (e.g., the difference in substrate availability between FL and PA fractions). A higher glycan niche width in PA than in FL was seen for some relatively rare taxa (Chloroflexota, Nitrospiraeota, Lentisphaeraeota, Gemmatimonadetota, Bacillota, and Acidobacteriota) (Wilcoxon–Mann–Whitney test, $p < 0.05$), but not for the abundant taxa (Figure 7). These rare taxa had more abundant CAZymes targeting algal cell wall-related compounds containing pectin, fucose, mannose, fucoidan and rhamnose, and other complex polysaccharides. Therefore, the high glycan niche for these relatively rare taxa in PA was related with that the estuary tends to have larger



particles (i.e., larger phytoplankton and detritus). $O_{i,k}$ index between Planctomycetota and Verrucomicrobiota in water was over 0.8 with the highest in the PA fraction (0.93) (Table 1), suggesting the high degree overlap of glycan niche for these two phylum communities. In addition, a moderate degree overlap index $O_{i,k}$ (0.5–0.8) was found among Planctomycetota, Verrucomicrobiota, Bacteroidota, and Gammaproteobacteria. At the genus level, the high degree overlap index was found between *Alteromonas* and *Pseudoalteromonas* (the mean of 0.75) and between *Rhodopirellula* and *Mariniblastus* (the mean of 0.73) in all water samples.

3.5. Niche difference of bacteria in CAZymes families-substrate specificities

3.5.1. Nitrogen-containing polysaccharide-specific bacterial communities

The glycan niche separations were found for the dominant taxa as shown in Figure 8 according to CAZymes families-substrate specificities (Supplementary Table S8). The main N-glycan-specific phyla were Alpha- and Gammaproteobacteria and Bacteroidota in water and Delta- and Gammaproteobacteria in sediment at the phylum level, respectively. At the genus level, *Candidatus Pelagibacter* is primarily associated with enzyme families (GH103, GH23, 73, 108, 24, and PL12) that encode the degradation of nitrogen-containing polysaccharides such as peptidoglycan and other amino sugars (Supplementary Figure S6A), with the highest contribution found in the free-living cells of the surface waters for GH73 (Wilcoxon–Mann–Whitney test, $p < 0.05$) (Figure 9A). In contrast, *Alteromonas* dominated GH23, 103, and 73 in bottom waters rather than in surface

waters (Wilcoxon–Mann–Whitney test, $p < 0.05$) (Figure 9A). With respect to the contributions of *Candidatus Pelagibacter* and *Alteromonas* to the total of GH23, 103, and 73 gene abundances, significant negative correlations were observed between these two genera for GH23 ($R^2 = 0.13$), GH103 ($R^2 = 0.75$) and GH73 ($R^2 = 0.88$) in water (Supplementary Figure S7). These negative correlations suggest a competitive relationship and a pronounced niche separation between *Candidatus Pelagibacter* and *Alteromonas* in the metabolism of nitrogen-containing polysaccharides occurred in the coastal zone of the PRE.

GH109 is a family of N-acetylhexosaminidase (an exoglycosidase that catalyzes the hydrolysis of terminal, non-reducing β -N-Acetylgalactosamine and glucosamine residues from oligosaccharides) targeting chondroitin sulfate, oligo-chitin, muramic acid, N-glycans attached to proteins and the other glycoconjugates. In addition, GH33 is acetylneuraminyl hydrolase with the hydrolysis function of glycoconjugates. Interestingly, the GH109 and GH33 family gene was highly enriched in anaerobic Planctomycetota, Bacteroidetes, and Verrucomicrobiota (Supplementary Figure S8). GH18 (chitinases) and GH20 (β -N-acetylglucosaminidase) are involved in the degradation of chitins, and AA10 (lytic polysaccharide monooxygenases, LPMOs) oxidize the crystalline chitin to produce chitooligosaccharides (Jiang et al., 2022). *Pseudoalteromonas* and *Vibrio* were the primary candidates for GH18, GH20 (Supplementary Figure S6A), and AA10 in this study. In the inner shelf of the PRE, $30.6 \pm 8.9\%$ of AA10 was assigned to *Pseudoalteromonas* in the particle-attached fraction suggesting the importance of Gammaproteobacteria *Pseudoalteromonas* in the initial degradation of crystalline chitin by oxidative pathway.

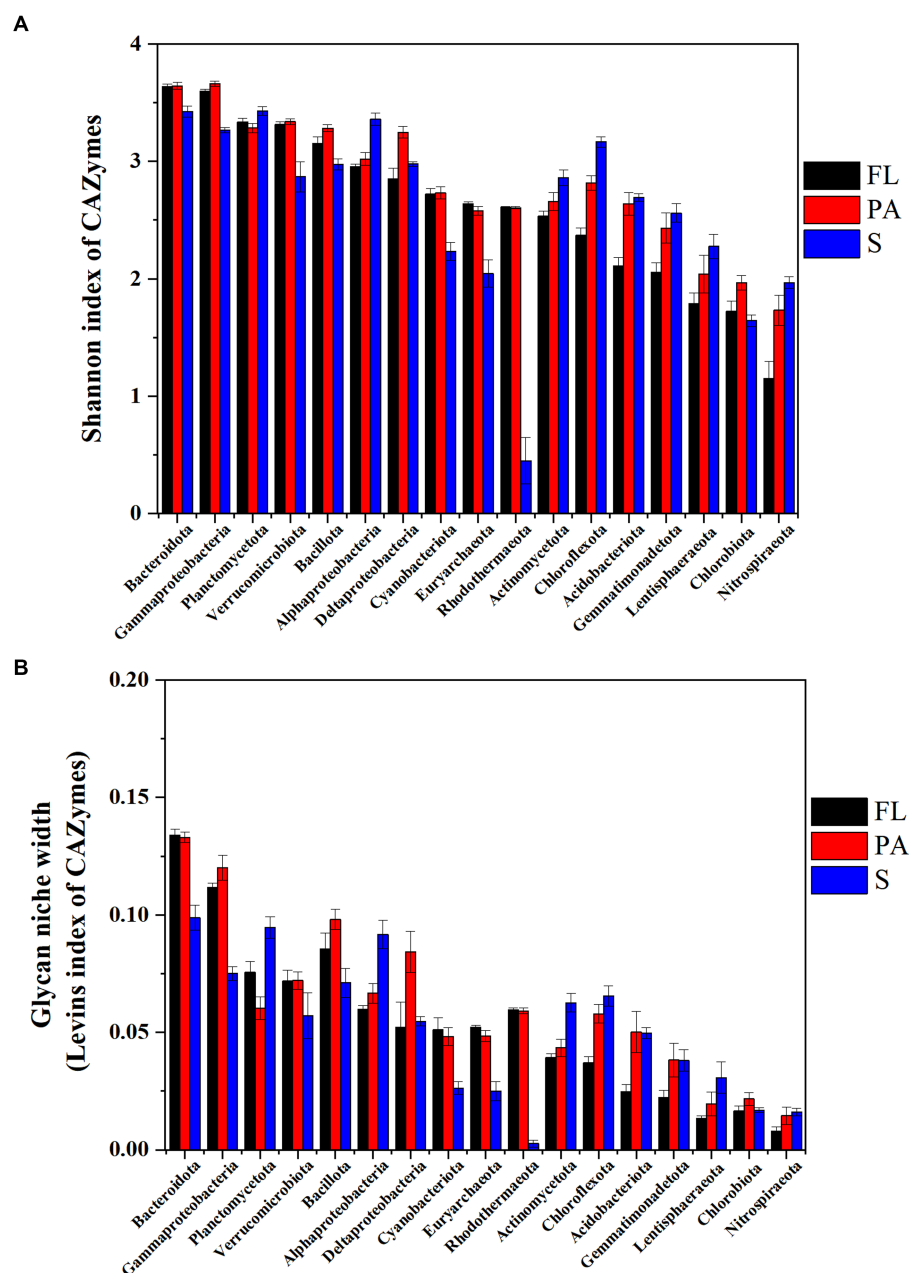


FIGURE 7

CAZymes diversity indicated by Shannon- index (A) and glycan niche width indicated by Levins index (B) (FL, free-living fraction; PA, particle-associated fraction; S, sediment).

3.5.2. Storage polysaccharide-specific bacterial communities

With respect to β -glucans, Bacteroidota and Gammaproteobacteria were the prominent phyla with laminarin (β -1, 3-glucans, the main storage polysaccharides in algae) degrading enzymes (Figure 8). Enzymes from different enzyme families process the laminarin degradation pathway. Endo-glucanases (GH16 and GH17) often cleave the backbone of laminarin (β -1,3-linked glucose main chain), and GH30 enzymes remove the β -1,6 side chain glucose. The obtained oligosaccharides are subsequently hydrolyzed into glucose by GH3, 1 and 5 enzymes, and other glucosidases. In water, the dominant genera containing GH16 enzyme genes were *Lewinella*, *haeodactylibacter*, and *Polaribacter* (Bacteroidota) (Supplementary Figure S6B). For

GH17 and GH30, *Formosa*, (a member of the family Flavobacteriaceae), was the dominant genus encoding for these two enzymes in water (Supplementary Figure S6B). The overwhelmingly dominant bacteria for oligo- β -glucan degradation (GH1 and GH3) were *Alteromonas* and *Candidatus Pelagibacter* in water (Supplementary Figure S6B). In addition, *Alteromonas* showed a significantly higher level of GH3 (25.3%) and GH1 (48.99%) in particle-associated bacteria of bottom waters than those in free-living fraction (Wilcoxon-Mann-Whitney test, $p < 0.05$) (Figure 9B). Besides Proteobacteria and Bacteroidota, the main storage polysaccharide-specific bacterial phyla were Actinomycetota (for α -glucan) in water and Chloroflexota (for α -glucan and β -glucan) and Nitrospiraeota (for α -glucan) in sediments, respectively. The CAZymes

TABLE 1 The overlap index ($O_{i,j}$) of glycan niches at the phylum level.

Free-living fractions	P1	P2	P3	P4	P5	P6	P7	P8	P9	P10	P11	P12	P13	P14	P15	P16	P17
P1/Acidobacterota	0.00																
P2/Actinobacterota	0.10	0.00															
P3/Armatimonadetota	0.05	0.04	0.00														
P4/Bacteroidetota	0.17	0.23	0.12	0.00													
P5/Candidatus Bathyarchaeota	0.00	0.00	0.00	0.00	0.00												
P6/Candidatus Marinimicrobiota	0.10	0.18	0.09	0.48	0.00	0.00											
P7/Chloroflexota	0.03	0.15	0.01	0.29	0.00	0.38	0.00										
P8/Cyanobacteria	0.19	0.44	0.15	0.37	0.00	0.30	0.16	0.00									
P9/Euryarchaeota	0.13	0.32	0.03	0.46	0.00	0.28	0.28	0.41	0.00								
P10/Bacillota	0.07	0.36	0.06	0.43	0.00	0.34	0.18	0.50	0.46	0.00							
P11/Gemmatimonadetota	0.10	0.37	0.07	0.31	0.03	0.48	0.25	0.60	0.53	0.50	0.00						
P12/Lentisphaerota	0.04	0.02	0.01	0.30	0.00	0.74	0.29	0.02	0.02	0.08	0.05	0.00					
P13/Nitrospirota	0.08	0.38	0.07	0.25	0.00	0.38	0.05	0.62	0.25	0.44	0.80	0.03	0.00				
P14/Planctomycetota	0.14	0.16	0.17	0.54	0.00	0.15	0.09	0.24	0.21	0.21	0.14	0.05	0.22	0.00			
P15/Proteobacteria	0.11	0.24	0.05	0.56	0.00	0.26	0.47	0.49	0.42	0.40	0.31	0.07	0.26	0.27	0.00		
P16/Rhodothermaeota	0.12	0.20	0.07	0.68	0.00	0.43	0.37	0.16	0.57	0.21	0.24	0.26	0.11	0.55	0.40	0.00	
P17/Verrucomicrobiota	0.14	0.25	0.08	0.56	0.00	0.19	0.12	0.40	0.28	0.38	0.32	0.05	0.42	0.80*	0.35	0.50	0.00
Particle-associated fractions	P1	P2	P3	P4	P5	P6	P7	P8	P9	P10	P11	P12	P13	P14	P15	P16	P17
P1/Acidobacterota	0.00																
P2/Actinobacterota	0.24	0.00															
P3/Armatimonadetota	0.20	0.01	0.00														
P4/Bacteroidetota	0.41	0.26	0.09	0.00													
P5/Candidatus Bathyarchaeota	0.00	0.00	0.00	0.00	0.00												
P6/Candidatus Marinimicrobiota	0.25	0.23	0.02	0.46	0.00	0.00											
P7/Chloroflexota	0.17	0.20	0.01	0.44	0.00	0.61	0.00										
P8/Cyanobacteria	0.33	0.39	0.04	0.31	0.00	0.37	0.17	0.00									
P9/Euryarchaeota	0.28	0.33	0.01	0.39	0.00	0.24	0.30	0.30	0.00								
P10/Bacillota	0.26	0.28	0.01	0.39	0.00	0.21	0.25	0.35	0.34	0.00							
P11/Gemmatimonadetota	0.37	0.34	0.04	0.46	0.02	0.50	0.33	0.51	0.41	0.32	0.00						
P12/Lentisphaerota	0.05	0.04	0.02	0.32	0.00	0.70	0.55	0.04	0.03	0.06	0.14	0.00					
P13/Nitrospirota	0.21	0.34	0.02	0.24	0.00	0.50	0.14	0.54	0.22	0.22	0.62	0.03	0.00				
P14/Planctomycetota	0.19	0.19	0.06	0.55	0.00	0.15	0.10	0.19	0.15	0.18	0.33	0.11	0.27	0.00			
P15/Proteobacteria	0.44	0.26	0.02	0.58	0.00	0.31	0.34	0.45	0.32	0.47	0.38	0.10	0.24	0.24	0.00		
P16/Rhodothermaeota	0.31	0.19	0.03	0.67	0.00	0.37	0.44	0.13	0.52	0.15	0.38	0.31	0.08	0.53	0.38	0.00	
P17/Verrucomicrobiota	0.18	0.19	0.06	0.59	0.00	0.17	0.11	0.25	0.19	0.23	0.41	0.11	0.31	0.93*	0.29	0.50	0.00
Sediment	P1	P2	P3	P4	P5	P6	P7	P8	P9	P10	P11	P12	P13	P14	P15	P16	P17

(Continued)

TABLE 1 (Continued)

Free-living fractions	P1	P2	P3	P4	P5	P6	P7	P8	P9	P10	P11	P12	P13	P14	P15	P16	P17
P1/Acidobacterota	0.00																
P2/Actinobacterota	0.59	0.00															
P3/Armatimonadetota	0.14	0.10	0.00														
P4/Bacteroidetota	0.26	0.49	0.30	0.00													
P5/Candidatus Bathyarchaeota	0.12	0.20	0.07	0.09	0.00												
P6/Candidatus Marinimicrobiota	0.00	0.00	0.00	0.01	0.00	0.00											
P7/Chloroflexota	0.32	0.43	0.08	0.42	0.25	0.00	0.00										
P8/Cyanobacteria	0.16	0.30	0.01	0.29	0.08	0.00	0.53	0.00									
P9/Euryarchaeota	0.12	0.32	0.01	0.25	0.09	0.00	0.08	0.03	0.00								
P10/Bacillota	0.19	0.21	0.17	0.16	0.11	0.00	0.31	0.15	0.01	0.00							
P11/Gemmatimonadetota	0.48	0.42	0.06	0.38	0.06	0.00	0.64	0.70	0.03	0.22	0.00						
P12/Lentisphaerota	0.03	0.01	0.07	0.09	0.02	0.12	0.02	0.01	0.01	0.02	0.04	0.00					
P13/Nitrospirota	0.23	0.32	0.00	0.24	0.00	0.00	0.49	0.72	0.01	0.20	0.75	0.00	0.00				
P14/Planctomycetota	0.21	0.31	0.23	0.41	0.45	0.00	0.13	0.05	0.22	0.22	0.11	0.14	0.06	0.00			
P15/Proteobacteria	0.50	0.34	0.06	0.31	0.13	0.00	0.44	0.33	0.20	0.21	0.49	0.03	0.46	0.20	0.00		
P16/Rhodothermaeota	0.31	0.13	0.00	0.06	0.00	0.00	0.12	0.00	0.00	0.04	0.34	0.00	0.03	0.00	0.12	0.00	
P17/Verrucomicrobiota	0.18	0.15	0.29	0.39	0.01	0.00	0.12	0.08	0.16	0.11	0.15	0.15	0.04	0.34	0.15	0.05	0.00

Moderate degree of overlap, $0.5 < O_{ik} < 0.5-0.8$; *high degree of overlap, $O_{ik} > 0.8$.

families GH13, 77, 15, 37, 97, 65, and CBM48 are involved in the degradation of α -linkages in glucan (e.g., starch and pullulan). At the genus level, *Alteromonas* dominated GH13 and 77 genes in water, specifically in the particle-attached bacterial fraction in bottom waters (Figure 9B), for example, 40.8% at MC01BP and 35.1% at DS02BP with respect to GH13. In the sediment, the dominant bacterial genus for degradation of α - and β - linked glucan were *Woeseia* due to their enrichment genes encoding GH13, GH77, CBM48, GH3, and GH 1 (Supplementary Figure S6B).

3.5.3. Hemicelluloses, celluloses, and lignin-specific bacterial communities

GH43 (β -xylosidase; α -L-arabinofuranosidase), GH2 (arabinosidases), GH5 (endo- β -1, 4-glucanase / cellulase; endo- β -1, 4-xylanase) are responsible for degradation of hemicelluloses and celluloses. CE1 targets a large variety of substrates including the deacetylation of xylan. Most GH43 was assigned to *Pseudoalteromonas*, and GH2 and CE1 were assigned to *Alteromonas*. *Candidatus Pelagibacter* dominated GH5 targeted for oligo-glucan (Supplementary Figure S6C). For lignin degradation, *Candidatus Pelagibacter* and *Alteromonas* were dominating the AA3 family (Supplementary Figure S6C) and AA6 genes. AA3 belongs to the glucose-methanol-choline (GMC) oxidoreductases family involved in lignocellulose degradation together with other AA-enzymes such as peroxidases (AA2). AA6 can be involved in the production of extracellular oxyradicals for lignin modification via Fenton action and subsequent break of the lignin barrier to enhance the binding of

CAZymes to lignocellulose. A high abundance of AA3, AA2, and GH2 families was found in *Alteromonas* only in bottom water samples, in particular in the particle-attached fraction (Wilcoxon–Mann–Whitney test, $p < 0.05$) (Figure 9B).

3.5.4. Acidic-polysaccharides-specific bacterial communities

Notably, *Alteromonas* was proved to be the specialist for degradation of pectinaceous polysaccharides, with PL1 (pectate lyase, cleaving α -(1, 4)-linked D-galacturonan), GH28 (both endo and exo acting polygalacturonases), GH105 (unsaturated glucuronyl/galacturonyl hydrolases), CE8 (pectinesterase), CE12 (pectin acetyltransferase) predominating (Supplementary Figure S6D). Furthermore, PL6, 7, and 17, which contain members catalyzing the depolymerization of alginate, were also dominated by *Alteromonas*. For example, the contribution of genes from *Alteromonas* to the gene abundance of PL6 were $32.34 \pm 13.17\%$, $26.71 \pm 14.15\%$, $76.59 \pm 15.32\%$, $91.76 \pm 2.61\%$ in SF (surface free-living fraction), SP (surface particle-associated fraction), BF (bottom free-living fraction), and BP (bottom particle-associated fraction), respectively (Supplementary Figure S6D).

Our results also showed that Flavobacteriales, Gammaproteobacteria, Planctomycetota, and Verrucomicrobiota played an important role in the debranching of fucose- and rhamnose-rich sulfated heteropolysaccharides (FRSP) in the coastal PRE (Figure 8). For the genes encoding the fucosidase GH29 family, the metagenomic results showed that *Polaribacter* (a member of the family Flavobacteriaceae) and *Halioglobus* (members of the class

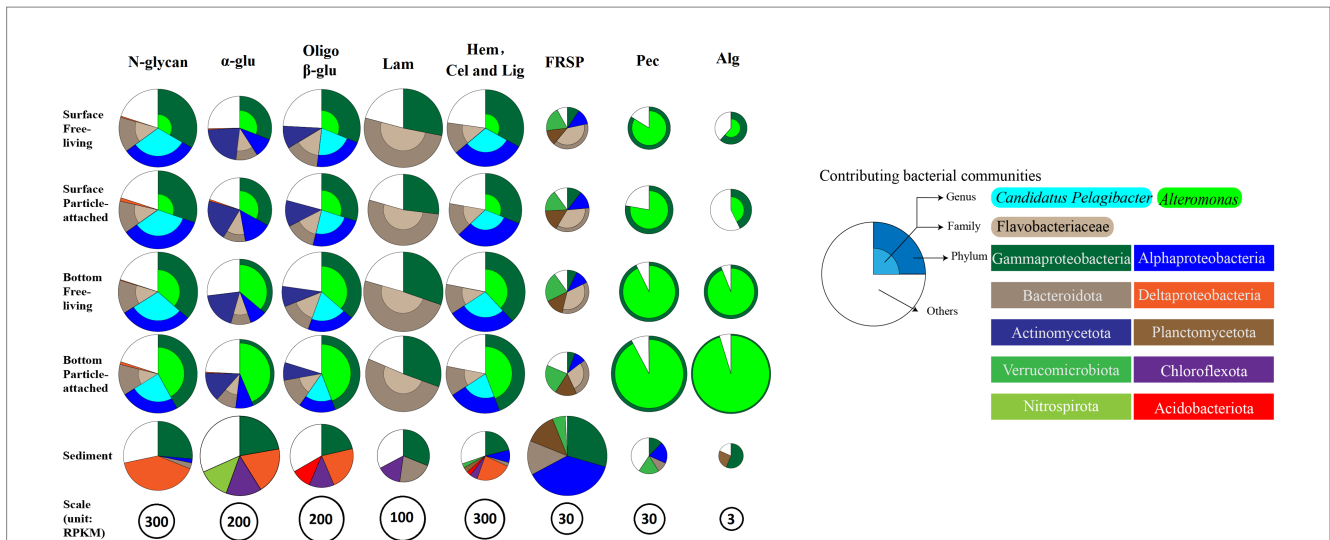


FIGURE 8
Glycan niches of dominant taxa in CAZymes families-substrate specificities in the inner shelf of the PRE (The specified functional categories of CAZymes are shown: (1) N-glycan, targeting nitrogen-containing polysaccharides; (2) α-glu, targeting α-linked glucan; (3) Oligo β-G, targeting oligo β-linked glucan; (4) Hem, Cel and Lig, targeting cellulose, hemicellulose and lignin; (5) FRSP, targeting sulfated fucose and rhamnose containing polysaccharides; (6) P, targeting pectin and pectate; (7) Alg, targeting alginate or alginic Acid).

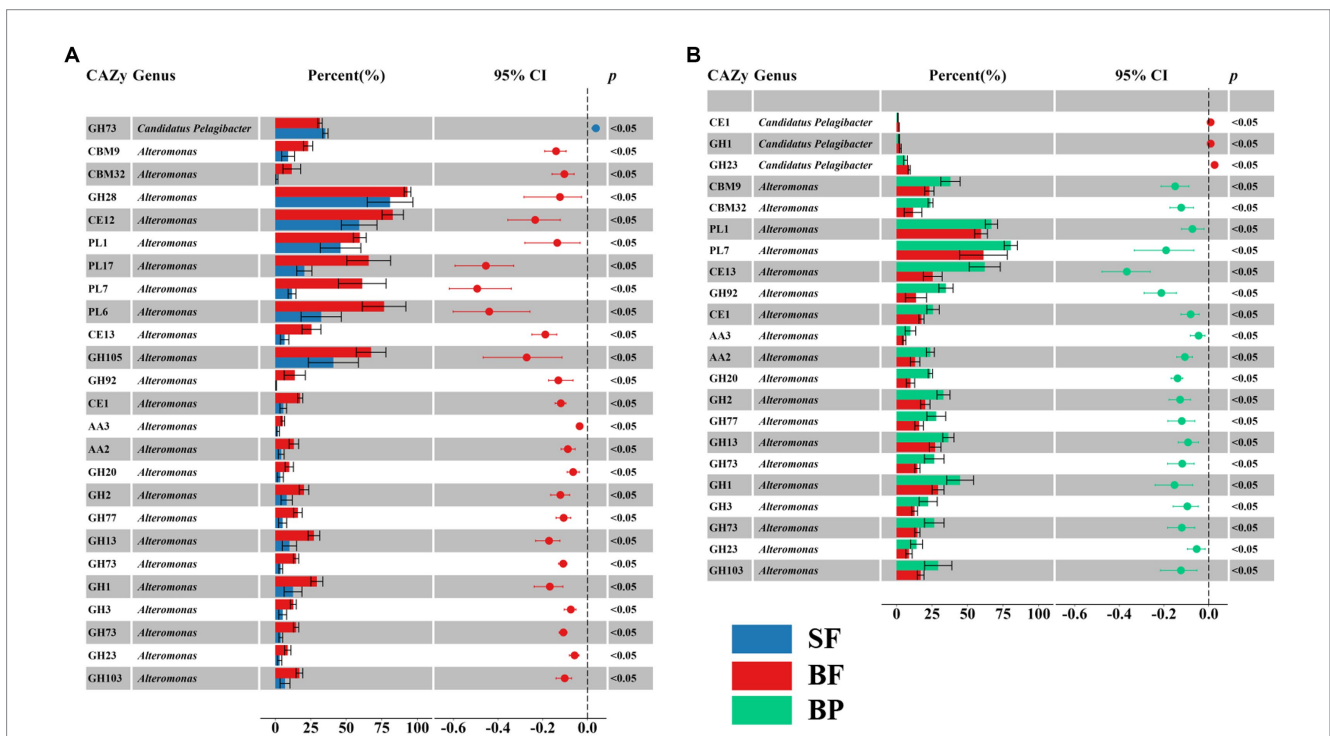


FIGURE 9
Significant difference in contributions of selective CAZymes abundance of *Alteromonas* and *Candidatus Pelagibacter* to the total CAZymes family abundance between surface free-living fraction (SF) and bottom free-living fraction (BF) (A), and between bottom particle-associated fraction and bottom free-living fraction (BF) (B).

Gammaproteobacteria) were the dominant genera, accounting for up to 12.17 and 9.24% of the total GH29 gene abundance in water, respectively (Supplementary Figure S6E). CBM47 (Fucose-binding activity) gene was rich in the Planctomycetota genera *Planctomyces* (12.94%) and *Rhodopirellula* (6.64%) in water. Furthermore, multiple sulfatase genes were detected in Flavobacteriales, Planctomycetales,

and Verrucomicrobiales (Supplementary Figure S9). Regarding rhamnose-rich heteropolysaccharides, the GH78 family (rhamnosidase) genes were significantly less abundant than the GH29 family genes in the metagenomes. *Candidatus Pelagibacter* were dominating the genes encoding the GH78 family except for samples of MC01BP and *Rhodopirellula* were dominating CBM67 (binding

rhamnose containing polysaccharide) in water, respectively. In the sediment, most GH29 genes were assigned to the *Halioglobus*, *Pseudoalteromonas* (Gammaproteobacteria), and *Colwellia* (Flavobacterium). The contributions of *Rhodopirellula* (Planctomycetota) to GH78 gene abundance were the highest with 16.60% at genus level in sediment (Supplementary Figure S6E).

3.6. Polymeric carbohydrate utilization mechanisms in different bacterial communities

In this study, the most dominant bacterial taxa involved in polysaccharide degradation were *Alteromonas*, *Candidatus Pelagibacter*, and the family Flavobacteriaceae. To better understand their carbohydrate uptake strategies, we additionally analyzed the carbohydrate transportation system in *Alteromonas*, *Candidatus Pelagibacter*, and Flavobacteriaceae. Generally, microbial transportation systems mainly include ATP-binding cassette (ABC) transporters (function for transportation of small molecular matter such as free amino acids and sugars), the phosphotransferase system (PTS), major facilitator super family (MFS) proton symporters, TonB-dependent receptors (TBDRs) and the starch utilization system C (SusC). The 'selfish bacterium' usually has genome encoding SusC transporters through which poly and oligo-saccharides come into the periplasm and then be hydrolyzed to monosaccharides for subsequent utilization with little loss of public products (oligosaccharides). In this study, SusC transporters and periplasmic protein TonB took most of the transportation system in Flavobacteriaceae (Table 2). Moreover, the presence of transporters (fucP, rhaP, and rhaQ, permease protein on fucose and rhamnose) (Table 2) and related CAZymes of the complex fucose- and rhamnose-containing polysaccharides in Flavobacteriaceae indicated that they were the specialists for consuming these polysaccharides in selfish mode, and were classed as moderate copiotrophs. This 'selfish' manner highly improves the payback of polysaccharide degradation enzymes. When substrates are sufficiently abundant, cells degrade polysaccharides to suitable sizes, providing extracellular hydrolysis products to the environment in sharing mode. Then, scavengers (beneficiaries) can directly take up the hydrolysis products created by the pioneers (Reintjes et al., 2020; Arnosti et al., 2021). In this study, the transporters in *Candidatus Pelagibacter* were all classified to the ABC transportation system, in which sugar transporters with low specificity took up the majority (Table 2). Moreover, the relative abundances (RPKM) of the transporter in *Candidatus Pelagibacter* are ten times as in *Alteromonas* and exhibited higher abundance in the free-living fractions than in the particle-attached bacteria (Table 2). Therefore, the scavenging mode by *Candidatus Pelagibacter* in free-living fractions through ABC transporters might be more prevalent and explain the dominance of *Candidatus Pelagibacter* for the assimilation of dissolved carbohydrates. Compared to *Candidatus Pelagibacter*, *Alteromonas* had a more complex transportation system, containing TonB, ABC, PTS, and MFS (Table 2). Due to the higher substrate specificity of TonB, PTS, and MFS than ABC (Lauro et al., 2009), *Alteromonas* may develop high efficiency in sugar transportation under copiotroph conditions, which enables *Alteromonas* to grow rapidly when nutrition is enough. This could explain the huge difference in the *Alteromonas* abundance between bottom and surface waters, particularly on

bottom particles, where substrates are likely available in sufficiently dense patches (Ebrahimi et al., 2019). The most diverse CAZymes and sugar transportation systems found for *Alteromonas* on particles in this study were consistent with heterogeneous carbohydrate-defined niches, which was also found for phytoplankton blooms in the North Sea and the coast of the northern South China Sea (Dong et al., 2014; Francis et al., 2021). Therefore, differences in CAZymes, substrate binding, and importing mechanisms of these dominant bacterial communities indicate glycan niche speciation and contrasting strategies in carbohydrate uptake in the PRE.

4. Discussion

Relative nutrient-poor status was found in the inner shelf of the PRE in winter, which has been found in a previous study (Liu et al., 2017). Previous studies in oceans and soils have found that nutrient levels and the availability of nutrients (i.e., organic carbon and nitrogen) determine the relative abundances of specific metabolic genes (Louca et al., 2016; Gowda et al., 2022). Therefore, the CAZymes gene frequency of Σ (GHs + CBMs + CEs + PLs) during this sampling time was comparable to the non-bloom phase at Helgoland (North Sea) (0.4–0.7% during non-bloom vs. 1.1% during bloom phase) (Teeling et al., 2016), coinciding with the low level of Chla concentration and poor nutrients status in this study.

In this study, CAZymes genes involved in the metabolism of nitrogen-containing polysaccharides contributed the largest proportions to the total abundance of GHs (Σ (GH23, 103, 108, 24, 73, 18, and 20), 34.04% in water and 24.61% in sediment, respectively). Moreover, PRKM of genes encoding lysozyme (GH73, 103, 108, 109, 24) on the coast of the PRE showed 3–4 times higher than those samples in non-bloom water in the North Sea at station approximately 60 km offshore from the northern German coastline, while the PRKM of most CAZymes families genes in this study were comparable to those samples (Vidal-Melgosa et al., 2021). Notably, an enzyme that degrades peptidoglycan that is not secreted is probably related to cell wall biosynthesis or recycling, but one that is secreted might be related to degrading environmental peptidoglycan (Vollmer et al., 2008; Gilmore and Cava, 2022). In the secreted CAZymes pool, GHs gene abundance [Σ (GH23, 103, 24, 73, 18, and 20)] also contributed the largest proportions to the total abundance of GHs, 36.27% in water and 53.30% in sediment, respectively (Supplementary Table S9). It was consistent with the results of a previous report that hydrolyses enzymes for degrading the polymer of N-actyl glucosamine dominated extracellular enzymatic activity at pristine offshore of PRE other than in eutrophic environments (Shi et al., 2019). Therefore, a high inventory of bacterial-derived necromass for microbial carbon turnover existed in the inner shelf of the PRE, due to a reduction in the supply of phytoplankton-derived organic matter in the coastal estuaries system in winter, coinciding with the low level of Chla concentration during the sampling time.

The α -diversity of CAZymes (Shannon index) in this study was lower than that of human gut microbes (Smits et al., 2017). Nevertheless, it was comparable to that of fungi in marine sediments (Baltar et al., 2021). In this study, the most abundant CAZymes and related genes and the widest glycan niche in the abundant bacterial taxa suggested their potential key roles in organic carbon utilization. *Alteromonas* were the most important genus according to both the

TABLE 2 Abundance (unit, RPKM) of transporters for different structure polysaccharides in *Alteromonas*, *Candidatus Pelagibacter*, and Flavobacteriaceae.

Bacterial taxa	Transporter	KO_ID	SF	SP	BF	BP	S
g_ <i>Alteromonas</i>	ABC.MS.S multiple sugar transport system substrate-binding protein	K02027	0.97	1.34	5.78	9.87	0.00
	fucP MFS transporter, FHS family, L-fucose permease	K02429	10.05	11.91	31.12	54.71	0.00
	lacY MFS transporter, OHS family, lactose permease	K02532	0.29	0.39	2.21	2.61	0.00
	PTS-Glc-EIIA, crr PTS system, sugar-specific IIA component	K02777	2.03	2.97	3.81	4.89	0.00
	tonB periplasmic protein TonB	K03832	13.50	15.83	31.87	47.90	0.00
g_ <i>Candidatus Pelagibacter</i>	ABC.MS.P multiple sugar transport system permease protein	K02025	36.58	32.45	36.30	28.25	0.08
	ABC.MS.P1 multiple sugar transport system permease protein	K02026	64.17	52.43	65.68	47.22	0.00
	ABC.MS.S multiple sugar transport system substrate-binding protein	K02027	128.22	73.63	128.79	91.25	0.08
	ABC.SS.A simple sugar transport system ATP-binding protein	K02056	129.27	107.43	135.73	97.68	0.70
	ABC.SS.P simple sugar transport system permease protein	K02057	153.16	107.41	159.41	116.30	0.09
	ABC.SS.S simple sugar transport system substrate-binding protein	K02058	122.79	65.39	120.38	84.05	0.00
	aglK alpha-glucoside transport system ATP-binding protein	K10235	1.18	0.68	0.69	0.60	0.00
	gtsA, glcE glucose/mannose transport system substrate-binding protein	K17315	17.94	10.55	18.64	12.52	0.00
	gtsB, glcF glucose/mannose transport system permease protein	K17316	4.70	3.54	4.85	3.50	0.00
	gtsC, glcG glucose/mannose transport system permease protein	K17317	34.01	26.53	35.69	26.99	0.02
	lacK lactose/L-arabinose transport system ATP-binding protein	K10191	5.11	4.42	5.62	4.95	0.00
	malK, mtlK, thuK multiple sugar transport system ATP-binding protein	K10111	9.73	8.83	9.55	8.23	0.04
f_ <i>Flavobacteriaceae</i>	ABC.MS.P1 multiple sugar transport system permease protein	K02026	0.15	0.11	0.19	0.09	0.00
	fucP MFS transporter, FHS family, L-fucose permease	K02429	5.05	5.66	5.19	3.88	1.29
	PTS-Fru2-EIIB PTS system, fructose-specific IIB-like component	K11202	0.49	0.35	0.50	0.13	0.00
	PTS-Fru-EIIA, fruB PTS system, fructose-specific IIA component	K02768	0.06	0.11	0.11	0.04	0.00
	PTS-Fru-EIIB, fruA PTS system, fructose-specific IIB component	K02769	0.19	0.39	0.26	0.31	0.00
	rhaP rhamnose transport system permease protein	K10560	0.37	0.15	0.37	0.21	0.00
	rhaQ rhamnose transport system permease protein	K10561	0.29	0.18	0.27	0.27	0.00
	susC TonB-dependent starch-binding outer membrane protein SusC	K21573	5.41	7.85	4.57	3.94	0.03
	tonB periplasmic protein TonB	K03832	5.64	8.35	3.94	2.76	1.25
	xylE MFS transporter, SP family, xylose:H ⁺ symportor	K08138	0.82	2.02	0.54	0.97	0.41

glycan niche index and microbial abundance followed by *Candidatus Pelagibacter* in this study. *Alteromonas* accounted for up to 22.19% of the total CAZymes gene abundance in the bottom water, which is nearly twice their proportions to the total microbial abundance. In addition, the composition of CAZymes of *Alteromonas* revealed that they are not only metabolic generalists capable of utilizing a wide variety of organic compounds (e.g., peptidoglycan, oligo- β -glucan, α -glucan, cellulose, hemicellulose), but also are specialists for recycling pectin and alginate. Similar results have been reported in experiments and *in situ* field observations indicating *Alteromonas* spp. comprised high proportional actively growing bacterial population (Pedler et al., 2014).

In contrast, the glycan niche of *Candidatus Pelagibacter* was narrower than those of *Alteromonas*. For example, no CBM family genes were detected in *Candidatus Pelagibacter*, although they contained abundant CAZymes genes (Figure 6A). CBMs are the most prominent ancillary modules and serve as non-catalytic accessory modules that bind carbohydrates, thus enhancing the catalytic efficiency of the multi-modular CAZymes (Boraston et al., 2004). The absence of CBMs genes in *Candidatus Pelagibacter* confirmed their oligotrophic niches, as they prefer to use the small molecule (i.e., one-carbon metabolism) rather than complex high molecular weight polysaccharides (Malmstrom et al., 2005; Tripp et al., 2008; Sun et al., 2011; Carini et al., 2014). Nevertheless, a large abundance of ABC transporters genes (multiple sugar transport system substrate-binding protein and simple sugar transport system ATP-binding protein) matched to *Candidatus Pelagibacter*, supported that they take up a substantial mono sugar or oligosaccharide from primary production or PG fragments mediated by ABC transporter in the oceans (Giovannoni, 2017; Noell et al., 2021; Gilmore and Cava, 2022). In addition, our results were consistent with previous reports that they have more genes for the uptake of amino acids and other nitrogenous compounds than for the uptake of carbohydrates (Cottrell and Kirchman, 2000; Noell et al., 2021). These findings suggest that *Alteromonas* and *Candidatus Pelagibacter* were the key genera for a significant flux of DOC and nutrient mineralization at the surface and the bottom, respectively, in this study (McCarren et al., 2010; Sun et al., 2011).

Bacteroidota and Gammaproteobacteria harbored remarkably abundant CAZymes genes for degrading laminarin. In particular, *Bacteroidota* contributed to over 50% of these genes (Figure 8). Laminarin (a food storage polysaccharide in diatoms) is a major component in the ocean and plays a prominent ecological role and biogeochemical function in oceanic carbon export and energy flow from primary production to next trophic levels in the food web (Becker et al., 2020). In this study, the relative abundance genes encoding GH16, 17, 30 (laminarinase) in the surface PA fraction was significantly lower than those in the FL fraction (Figure 4). It implies that "particulate" laminarin was better prevented from enzymatic hydrolysis and dissolution within the intact diatom cells. In contrast, the dissolved laminarin released from diatom can be quickly hydrolyzed by extracellular laminarinase, but also by 'selfish' uptake by *Bacteroidota* cells with little diffusive loss (Reintjes et al., 2020). It also indicated that DOM quality plays a significant role in controlling the microbial community response (Liu S. T. et al., 2020; Kieft et al., 2021). Fucose- and rhamnose-rich anionic heteropolysaccharides, which are also found in TEP (Passow, 2002), can show extensive sulphation. Due to their complex structure, they are rather recalcitrant and are degraded

more slowly (turnover time up to 1 month) than other polysaccharides, such as carbonylated polysaccharides α -1,4-galacturonan (turnover time of days to weeks) and β -1,3-glucan (turnover time of days) (Vidal-Melgosa et al., 2021). Previously, Planctomycetota were shown to colonize the surfaces of particles in the PRE, such as the diatom *Thalassiosira weissflogii* (Zhang et al., 2016; Ma et al., 2022). Thus, their enrichment of sulfatase (Supplementary Figure S9) and CBM genes in the surface water particle-attached fraction may be associated with the presence of fucose- and rhamnose-rich anionic sulfated heteropolysaccharides that are likely derived from phytoplankton in these samples. The results of this study were consistent with earlier findings on the degradation of anionic sulfated heteropolysaccharides by Flavobacteriales, Gamma-proteobacteria, Verrucomicrobiota and Planctomycetota (Wegner et al., 2013; King et al., 2015; Ma et al., 2022; Orellana et al., 2022). Furthermore, the CAZymes gene compositions revealed a close connection between microbiome and algae, which enable these communities to efficiently utilize carbohydrate carbon produced from algae (Gugi et al., 2015; Reintjes et al., 2019; Ma et al., 2022).

In this study, the vertical distribution reflected the difference in niches between layers and provided insights into carbon turnover and preservation. High abundance genes encoding α -glucosidases (GH13 and GH77) in sediment suggested that α -linked glucans (starch or pullulan) generally from algal, bacterial, and animal storage can be taken more rapid hydrolysis in sediment than in water. Similarly, rapid pullulan (α -linked glucans) degradation has also been found in all oxic and anoxic sediments from locations including the Baltic Sea, the eastern North Atlantic, and the Arctic Ocean (Arnosti, 2000). Furthermore, the significantly higher relative abundance of genes in sediment soil was found for fucosidases (GH 29 and 95), rhamnosidase (GH78, 106, and 145), and β -mannosides (GH130 and 26) involved in the utilization of cell wall polysaccharides (e.g., FRSP) compared to their abundances in water. These are enzymes for the hydrolysis of methyl pentose sugars, which are known as a potential carbon sink due to their challenge to degrading structure for bacteria compared to other monomers (Vidal-Melgosa et al., 2021). Generally, FRSP that diatoms secrete remains outside the cell or as part of the cell wall, and thus FRSP in POM also increases during the diatom bloom or post-bloom (Vidal-Melgosa et al., 2021). It has been suggested that increasing the concentration of secreted adhesive polysaccharides (TEP and their precursor) favors the aggregation of diatoms, accelerating their sinking velocity (Engel et al., 2004). This may explain the accumulation of FRSP in shallow sediments of the coast of the estuary during this study. The vertical distribution of GHs genes abundances further points to the selective degradation of polysaccharides with different bioavailability and that FRSP undergoes an extensive transformation in sediment rather than in water (Smith et al., 2019). Furthermore, RPKM of the PLs and GHs for acid polysaccharides were an order of magnitude below those of abundant GHs, CEs, and AAs targeting other substrates, indicating that acid polysaccharides might play a minor role in carbon turnover than nitrogen-containing polysaccharides, glucan, xylan, and lignin in the PRE inner shelf (Sun et al., 2012; Vidal-Melgosa et al., 2021).

With respect to the glycan overlap index, the high degree overlap of CAZymes was found between Planctomycetota and Verrucomicrobiota at the phylum level. At the genus level, the high degree overlap index was found between *Alteromonas* and *Pseudoalteromonas* and between *Rhodopirellula* and *Mariniblastus* in

all water samples. These species pairs were close relatives based on phylogenetic analysis (Gauthier et al., 1995; Butler et al., 2007; Munoz et al., 2016). Therefore, carbohydrate preferences are more similar with increasing phylogenetic relatedness, since more closely related strains tend to have more similar metabolic profiles (Bryson et al., 2017; Fahimipour and Gross, 2020; Kieft et al., 2021). However, a higher overlap index means a competitive relationship for carbohydrate utilization. The paradox that species with similar glycan niches tend to co-occur can be explained by deterministic environmental filtering (Santillan and Wuertz, 2022). A specific environment that provides some set of resources will be occupied by species that demand these resources, whereas a different set of species will fit a different environment offering a different set of nutrients (Levy and Borenstein, 2013). The similar utilization of diatom-produced polysaccharides (i.e., sulfated polysaccharide) determined glycan niche overlap among these taxa (Planctomycetota, Bacteroidota, Verrucomicrobiota, Gammaproteobacteria). In this study, the abundance of *Alteromonas* was higher than those of *Pseudoalteromonas*, indicating low-level co-occurrence degree although they had similar CAZymes structures. It has been found that *Alteromonas* have a faster N uptake ability than *Pseudoalteromonas* (Arandia-Gorostidi et al., 2022), suggesting that N-poor status in this study might reduce the competitiveness of *Pseudoalteromonas*. Therefore, the deterministic processes played an important role in microbiome assembly (Teeling et al., 2016).

5. Conclusion

This study offers insight into the mechanisms of microbial communities to degrade polymeric carbohydrates in the inner shelf of the estuarine system. In this study, nutrients and Chl *a* indicated relative nutrient-poor status during the sampling time, inducing a high fraction of GHs genes targeting peptidoglycan (bacterial cell wall) and chitin. Furthermore, significant differences in CAZymes profiles were found between water and sediment and between free-living and particle-attached bacterial fractions in water. The vertical distribution of CAZymes genes suggested a selective degradation of polysaccharides with different bioavailability, and a higher degree of recalcitrant FRSP biotransformation in sediment rather than in water. Proteobacteria and Bacteroidota had the highest abundance and glycan niche width of CAZymes in water, respectively. Members of the Alphaproteobacteria (*Candidatus Pelagibacter*), Gammaproteobacteria (*Alteromonas*, *Pseudoalteromonas*, and *Woeseia*), and Flavobacteriaceae were among the most prominent responders to the polymer carbohydrates. At the genus level, the glycan niches width of the genus *Alteromonas* were the widest for degradation of laminarin, starch, and nitrogen-containing polysaccharides, carboxylic-acid polysaccharides, cellulose, and lignin, associated multiple sugar transporter in sharing modal, and marked with depth difference (BF>SF) for free-living fraction and size difference for bottom samples (BP>BF). While the functional potentials of *Candidatus Pelagibacter* showed dominance for substrates like oligo-glucan, nitrogen-containing polysaccharides, oligo-cellulose, and lignin-derived aromatic fragments. The most abundant CAZymes and related genes and the widest glycan niche in the abundant bacterial taxa suggested their potential key roles in organic carbon utilization. The high extent of glycan niche overlap for utilization of diatom-produced polysaccharides revealed a close connection between

bacteria (e.g., Bacteroidota, Gammaproteobacteria, Planctomycetota, and Verrucomicrobiota) and algae. Collectively, CAZymes gene traits and their related transporters as a good proxy for assessing distinct 'polymeric carbohydrate utilization types' of the microbial communities indicated different bacterial strategies of polysaccharide degradation and the niches separation subject to polymeric carbohydrate substrates in the estuarine system.

Data availability statement

The datasets presented in this study can be found in online repositories. The names of the repository/repositories and accession number(s) can be found in the article/Supplementary material.

Author contributions

C-CS designed the manuscript and discussed the results and implications, and commented on the manuscript at all stages. W-JZ performed the annotation of the metagenome data and drew the figures, and did the sampling and chemical parameter analysis. Y-SW provided the research direction. W-ZY, HC, F-LS, Y-TW, M-LW, and AE helped to check the manuscript. All authors contributed to the article and approved the submitted version.

Funding

This study was supported by the National Natural Science Foundation of China (Nos. 42073078 and U1901211), Independent Research Project of State Key Laboratory of Tropical Oceanography (LTOZZ2202), the Key Research and Development Program of Hainan Province (ZDYF2021XDNY131), and the Strategic Priority Research Program of the Chinese Academy of Sciences (No. XDA19060204).

Conflict of interest

The authors declare that the research was conducted in the absence of any commercial or financial relationships that could be construed as a potential conflict of interest.

Publisher's note

All claims expressed in this article are solely those of the authors and do not necessarily represent those of their affiliated organizations, or those of the publisher, the editors and the reviewers. Any product that may be evaluated in this article, or claim that may be made by its manufacturer, is not guaranteed or endorsed by the publisher.

Supplementary material

The Supplementary material for this article can be found online at: <https://www.frontiersin.org/articles/10.3389/fmicb.2023.1180321/full#supplementary-material>

References

- Alderkamp, A. C., Van Rijssel, M., and Bolhuis, H. (2007). Characterization of marine bacteria and the activity of their enzyme systems involved in degradation of the algal storage glucan laminarin. *FEMS Microbiol. Ecol.* 59, 108–117. doi: 10.1111/j.1574-6941.2006.00219.x
- Aramaki, T., Blanc-Mathieu, R., Endo, H., Ohkubo, K., Kanehisa, M., Goto, S., et al. (2020). KofamKOALA: KEGG Ortholog assignment based on profile HMM and adaptive score threshold. *Bioinformatics* 36, 2251–2252. doi: 10.1093/bioinformatics/btz859
- Arandia-Gorostidi, N., Berthelot, H., Calabrese, F., Stryhanyuk, H., Klawonn, I., Iversen, M., et al. (2022). Efficient carbon and nitrogen transfer from marine diatom aggregates to colonizing bacterial groups. *Sci. Rep.* 12:14949. doi: 10.1038/s41598-022-18915-0
- Arnosti, C. (2000). Substrate specificity in polysaccharide hydrolysis: contrasts between bottom water and sediments. *Limnol. Oceanogr.* 45, 1112–1119. doi: 10.4319/lo.2000.45.5.1112
- Arnosti, C., Wietz, M., Brinkhoff, T., Hehemann, J. H., Probandt, D., Zeugner, L., et al. (2021). The biogeochemistry of marine polysaccharides: sources, inventories, and bacterial drivers of the carbohydrate cycle. *Annu. Rev. Mar. Sci.* 13, 81–108. doi: 10.1146/annurev-marine-032020-012810
- Avcı, B., Kruger, K., Fuchs, B. M., Teeling, H., and Amann, R. I. (2020). Polysaccharide niche partitioning of distinct Polaribacter clades during North Sea spring algal blooms. *ISME J.* 14, 1369–1383. doi: 10.1038/s41396-020-0601-y
- Baker, B. J., Lazar, C. S., Teske, A. P., and Dick, G. J. (2015). Genomic resolution of linkages in carbon, nitrogen, and sulfur cycling among widespread estuary sediment bacteria. *Microbiome* 3:14. doi: 10.1186/s40168-015-0077-6
- Baltar, F., Zhao, Z. H., and Herndl, G. J. (2021). Potential and expression of carbohydrate utilization by marine fungi in the global ocean. *Microbiome* 9:106. doi: 10.1186/s40168-021-01063-4
- Bankevich, A., Nurk, S., Antipov, D., Gurevich, A. A., Dvorkin, M., Kulikov, A. S., et al. (2012). SPAdes: a new genome assembly algorithm and its applications to single-cell sequencing. *J. Comput. Biol.* 19, 455–477. doi: 10.1089/cmb.2012.0021
- Barbeyron, T., Brillet-Gueguen, L., Carre, W., Carriere, C., Caron, C., Czjzek, M., et al. (2016). Matching the diversity of sulfated biomolecules: creation of a classification database for sulfatases reflecting their substrate specificity. *PLoS One* 11:e0164846. doi: 10.1371/journal.pone.0164846
- Becker, S., Tebben, J., Coffinet, S., Wiltshire, K., Iversen, M. H., Harder, T., et al. (2020). Laminarin is a major molecule in the marine carbon cycle. *Proc. Natl. Acad. Sci. U. S. A.* 117, 6599–6607. doi: 10.1073/pnas.1917001117
- Benner, R. (2002). “Chemical composition and reactivity” in *Biogeochemistry of marine dissolved organic matter*. ed. D. A. A. C. Hansell, C (San Diego, CA, USA: Academic Press, Elsevier Science)
- Benner, R. (2004). What happens to terrestrial organic matter in the ocean? *Mar. Chem.* 92, 307–310. doi: 10.1016/j.marchem.2004.06.033
- Benner, R., and Kaiser, K. (2011). Biological and photochemical transformations of amino acids and lignin phenols in riverine dissolved organic matter. *Biogeochemistry* 102, 209–222. doi: 10.1007/s10533-010-9435-4
- Bolger, A. M., Lohse, M., and Usadel, B. (2014). Trimmomatic: a flexible trimmer for Illumina sequence data. *Bioinformatics* 30, 2114–2120. doi: 10.1093/bioinformatics/btu170
- Boraston, A. B., Bolam, D. N., Gilbert, H. J., and Davies, G. J. (2004). Carbohydrate-binding modules: fine-tuning polysaccharide recognition. *Biochem. J.* 382, 769–781. doi: 10.1042/BJ20040892
- Bryson, S., Li, Z., Chavez, F., Weber, P. K., Pett-Ridge, J., Hettich, R. L., et al. (2017). Phylogenetically conserved resource partitioning in the coastal microbial loop. *ISME J.* 11, 2781–2792. doi: 10.1038/ismej.2017.128
- Buchfink, B., Xie, C., and Huson, D. H. (2015). Fast and sensitive protein alignment using DIAMOND. *Nat. Methods* 12, 59–60. doi: 10.1038/nmeth.3176
- Butler, M. K., Den Camp, H. J. M. O., Harhangi, H. R., Lafi, F. F., Strous, M., and Fuerst, J. A. (2007). Close relationship of RNase P RNA in Gemmata and anammox planctomycete bacteria. *FEMS Microbiol. Lett.* 268, 244–253. doi: 10.1111/j.1574-6968.2006.00597.x
- Carini, P., White, A. E., Campbell, E. O., and Giovannoni, S. J. (2014). Methane production by phosphate-starved SAR11 chemoheterotrophic marine bacteria. *Nat. Commun.* 5:4346. doi: 10.1038/ncomms5346
- Costa, O. Y. A., De Hollander, M., Pijl, A., Liu, B. B., and Kuramae, E. E. (2020). Cultivation-independent and cultivation-dependent metagenomes reveal genetic and enzymatic potential of microbial community involved in the degradation of a complex microbial polymer. *Microbiome* 8:76. doi: 10.1186/s40168-020-00836-7
- Cottrell, M. T., and Kirchman, D. L. (2000). Natural assemblages of marine proteobacteria and members of the Cytophaga-Flavobacter cluster consuming low- and high-molecular-weight dissolved organic matter. *Appl. Environ. Microbiol.* 66, 1692–1697. doi: 10.1128/AEM.66.4.1692-1697.2000
- Cuskin, F., Lowe, E. C., Temple, M. J., Zhu, Y. P., Cameron, E. A., Pudlo, N. A., et al. (2015). Human gut Bacteroidetes can utilize yeast mannan through a selfish mechanism. *Nature* 520:388. doi: 10.1038/nature14334
- Dal Bello, M., Lee, H., Goyal, A., and Gore, J. (2021). Resource-diversity relationships in bacterial communities reflect the network structure of microbial metabolism. *Nat. Ecol. Evol.* 5:1463. doi: 10.1038/s41559-021-01563-4
- Davis, M. P. A., Van Dongen, S., Abreu-Goodger, C., Bartonicek, N., and Enright, A. J. (2013). Kraken: a set of tools for quality control and analysis of high-throughput sequence data. *Methods* 63, 41–49. doi: 10.1016/j.ymeth.2013.06.027
- Dong, H. P., Hong, Y. G., Lu, S. H., and Xie, L. Y. (2014). Metaproteomics reveals the major microbial players and their biogeochemical functions in a productive coastal system in the northern South China Sea. *Environ. Microbiol. Rep.* 6, 683–695. doi: 10.1111/1758-2229.12188
- Ebrahimi, A., Schwartzman, J., and Cordero, O. X. (2019). Cooperation and spatial self-organization determine rate and efficiency of particulate organic matter degradation in marine bacteria. *Proc. Natl. Acad. Sci. U. S. A.* 116, 23309–23316. doi: 10.1073/pnas.1908512116
- Engel, A., Thoms, S., Riebesell, U., Rochelle-Newall, E., and Zondervan, I. (2004). Polysaccharide aggregation as a potential sink of marine dissolved organic carbon. *Nature* 428, 929–932. doi: 10.1038/nature02453
- Fahimipour, A. K., and Gross, T. (2020). Mapping the bacterial metabolic niche space. *Nature Communications* 11:4887. doi: 10.1038/s41467-020-18695-z
- Francis, B., Urich, T., Mikolasch, A., Teeling, H., and Amann, R. (2021). North Sea spring bloom-associated Gammaproteobacteria fill diverse heterotrophic niches. *Environ. Microbiome* 16:15. doi: 10.1186/s40793-021-00385-y
- Garza, D. R., Van Verk, M. C., Huynen, M. A., and Dutilh, B. E. (2018). Towards predicting the environmental metabolome from metagenomics with a mechanistic model. *Nat. Microbiol.* 3, 456–460. doi: 10.1038/s41564-018-0124-8
- Gauthier, G., Gauthier, M., and Christen, R. (1995). Phylogenetic analysis of the genera *Alteromonas*, *Shewanella*, and *Moritella* using genes coding for small-subunit rRNA sequences and division of the genus *Alteromonas* into two genera, *Alteromonas* (emended) and *Pseudoalteromonas* gen. nov., and proposal of twelve new species combinations. *Int. J. Syst. Evol. Microbiol.* 45, 755–761.
- Gilmore, M. C., and Cava, F. (2022). Peptidoglycan recycling mediated by an ABC transporter in the plant pathogen *Agrobacterium tumefaciens*. *Nat. Commun.* 13:7927. doi: 10.1038/s41467-022-35607-5
- GINestet, C. (2011). ggplot2: elegant graphics for data analysis. *J. R. Stat. Soc. A Stat. Soc.* 174, 245–246. doi: 10.1111/j.1467-985X.2010.00676_9.x
- Giovannoni, S. J. (2017). SAR11 bacteria: the most abundant plankton in the oceans. *Annu. Rev. Mar. Sci.* 9, 231–255. doi: 10.1146/annurev-marine-010814-015934
- Gowda, K., Ping, D., Mani, M., and Kuehn, S. (2022). Genomic structure predicts metabolic dynamics in microbial communities. *Cells* 185:530. doi: 10.1016/j.cell.2021.12.036
- Gugi, B., Le Costaouec, T., Burel, C., Lerouge, P., Helbert, W., and Bardor, M. (2015). Diatom-specific oligosaccharide and polysaccharide structures help to unravel biosynthetic capabilities in diatoms. *Mar. Drugs* 13, 5993–6018. doi: 10.3390/md13095993
- Hallgren, J., Tsigiris, K. D., Pedersen, M. D., Armenteros, J. J. A., Marcatili, P., Nielsen, H., et al. (2022). DeepTMHMM predicts alpha and beta transmembrane proteins using deep neural networks. *bioRxiv*. doi: 10.1101/2022.04.08.487609
- He, B., Dai, M., Huang, W., Liu, Q., Chen, H., and Xu, L. (2010a). Sources and accumulation of organic carbon in the Pearl River Estuary surface sediment as indicated by elemental, stable carbon isotopic, and carbohydrate compositions. *Biogeosciences* 7, 3343–3362. doi: 10.5194/bg-7-3343-2010
- He, B., Dai, M. H., Zhai, W. D., Wang, L. F., Wang, K. J., Chen, J. H., et al. (2010b). Distribution, degradation and dynamics of dissolved organic carbon and its major compound classes in the Pearl River Estuary, China. *Mar. Chem.* 119, 52–64. doi: 10.1016/j.marchem.2009.12.006
- Hehemann, J. H., Truong, L. V., Unfried, F., Welsch, N., Kabisch, J., Heiden, S. E., et al. (2017). Aquatic adaptation of a laterally acquired pectin degradation pathway in marine gammaproteobacteria. *Environ. Microbiol.* 19, 2320–2333. doi: 10.1111/1462-2920.13726
- Herold, M., Arbas, S. M., Narayanasamy, S., Sheik, A. R., Kleine-Borgmann, L. A. K., Lebrun, L. A., et al. (2020). Integration of time-series meta-omics data reveals how microbial ecosystems respond to disturbance. *Nat. Commun.* 11:5281. doi: 10.1038/s41467-020-19006-2
- Hung, C. C., Tang, D. G., Warnken, K. W., and Santschi, P. H. (2001). Distributions of carbohydrates, including uronic acids, in estuarine waters of Galveston Bay. *Mar. Chem.* 73, 305–318. doi: 10.1016/S0304-4203(00)00114-6
- Hyatt, D., Chen, G. L., Locascio, P. F., Land, M. L., Larimer, F. W., and Hauser, L. J. (2010). Prodigal: prokaryotic gene recognition and translation initiation site identification. *BMC Bioinform.* 11:119. doi: 10.1186/1471-2105-11-119
- Jiang, W. X., Li, P. Y., Chen, X. L., Zhang, Y. S., Wang, J. P., Wang, Y. J., et al. (2022). A pathway for chitin oxidation in marine bacteria. *Nat. Commun.* 13:5899. doi: 10.1038/s41467-022-33566-5
- Jiao, N. Z., Herndl, G. J., Hansell, D. A., Benner, R., Kattner, G., Wilhelm, S. W., et al. (2011). The microbial carbon pump and the oceanic recalcitrant dissolved organic matter pool. *Nat. Rev. Microbiol.* 9:555. doi: 10.1038/nrmicro2386-c5

- Kieft, B., Li, Z., Bryson, S., Hettich, R. L., Pan, C., Mayali, X., et al. (2021). Phytoplankton exudates and lysates support distinct microbial consortia with specialized metabolic and ecophysiological traits. *Proc. Natl. Acad. Sci.* 118:e2101178118. doi: 10.1073/pnas.2101178118
- Kits, K. D., Sedlacek, C. J., Lebedeva, E. V., Han, P., Bulaev, A., Pjevac, P., et al. (2017). Kinetic analysis of a complete nitrifier reveals an oligotrophic lifestyle. *Nature* 549:269–+. doi: 10.1038/nature23679
- Kuang, J. L., Huang, L. N., Chen, L. X., Hua, Z. S., Li, S. J., Hu, M., et al. (2013). Contemporary environmental variation determines microbial diversity patterns in acid mine drainage. *ISME J.* 7, 1038–1050. doi: 10.1038/ismej.2012.139
- Langmead, B., and Salzberg, S. L. (2012). Fast gapped-read alignment with bowtie 2. *Nat. Methods* 9, 357–359. doi: 10.1038/nmeth.1923
- Lauro, F. M., Mcdougald, D., Thomas, T., Williams, T. J., Egan, S., Rice, S., et al. (2009). The genomic basis of trophic strategy in marine bacteria. *Proc. Natl. Acad. Sci. U. S. A.* 106, 15527–15533. doi: 10.1073/pnas.0903507106
- Lazar, C. S., Baker, B. J., Seitz, K., Hyde, A. S., Dick, G. J., Hinrichs, K. U., et al. (2016). Genomic evidence for distinct carbon substrate preferences and ecological niches of Bathyarchaeota in estuarine sediments. *Environ. Microbiol.* 18, 1200–1211. doi: 10.1111/1462-2920.13142
- Levy, R., and Borenstein, E. (2013). Metabolic modeling of species interaction in the human microbiome elucidates community-level assembly rules. *Proc. Natl. Acad. Sci. U. S. A.* 110, 12804–12809. doi: 10.1073/pnas.1300926110
- Liu, S. T., Baetge, N., Comstock, J., Opalk, K., Parsons, R., Halewood, E., et al. (2020). Stable isotope probing identifies bacterioplankton lineages capable of utilizing dissolved organic matter across a range of bioavailability. *Front. Microbiol.* 11:580397. doi: 10.3389/fmicb.2020.580397
- Liu, H., Huang, L., Tan, Y., Zhixin, K. E., Liu, J., Zhao, C., et al. (2017). Seasonal variations of chlorophyll a and primary production and their influencing factors in the Pearl River Estuary. *J. Trop. Oceanogr.*
- Liu, Y. Y., Lin, Q., Feng, J. R., Yang, F. M., Du, H., Hu, Z., et al. (2020). Differences in metabolic potential between particle-associated and free-living bacteria along Pearl River Estuary. *Sci. Total Environ.* 728:138856. doi: 10.1016/j.scitotenv.2020.138856
- Louca, S., Parfrey, L. W., and Doebeli, M. (2016). Decoupling function and taxonomy in the global ocean microbiome. *Science* 353, 1272–1277. doi: 10.1126/science.aaf4507
- Luis, A. S., Basle, A., Byrne, D. P., Wright, G. S. A., London, J. A., Jin, C. S., et al. (2022). Sulfated glycan recognition by carbohydrate sulfatases of the human gut microbiota. *Nat. Chem. Biol.* 18:1032. doi: 10.1038/s41589-022-01132-1
- Ma, X., Johnson, K. B., Gu, B., Zhang, H., Li, G., Huang, X., et al. (2022). The in-situ release of algal bloom populations and the role of prokaryotic communities in their establishment and growth. *Water Res.* 219:118565. doi: 10.1016/j.watres.2022.118565
- Malmstrom, R. R., Cottrell, M. T., Elifantz, H., and Kirchman, D. L. (2005). Biomass production and assimilation of dissolved organic matter by SAR11 bacteria in the Northwest Atlantic Ocean. *Appl. Environ. Microbiol.* 71, 2979–2986. doi: 10.1128/AEM.71.6.2979-2986.2005
- Mccarren, J., Becker, J. W., Repeta, D. J., Shi, Y. M., Young, C. R., Malmstrom, R. R., et al. (2010). Microbial community transcriptomes reveal microbes and metabolic pathways associated with dissolved organic matter turnover in the sea. *Proc. Natl. Acad. Sci. U. S. A.* 107, 16420–16427. doi: 10.1073/pnas.1010732107
- Munoz, R., Rosselló-Móra, R., and Amann, R. (2016). Revised phylogeny of Bacteroidetes and proposal of sixteen new taxa and two new combinations including *Rhodothermaeota* phyl. nov. *Syst. Appl. Microbiol.* 39, 281–296. doi: 10.1016/j.syapm.2016.04.004
- Mykkestad, S. M., and Børshheim, K. Y. (2007). Dynamics of carbohydrates in the Norwegian Sea inferred from monthly profiles collected during 3 years at 66°N, 2°E. *Mar. Chem.* 107, 475–485. doi: 10.1016/j.marchem.2007.09.002
- Noell, S. E., Barrell, G. E., Suffridge, C., Morrè, J., Gable, K. P., Graff, J. R., et al. (2021). SAR11 cells rely on enzyme multifunctionality to transport and metabolize a range of polyamine compounds. *mBio.* 12:e0109121. doi: 10.1128/mBio.01091-21
- Oksanen, J., Simpson, G., Blanchet, F. G., Kindt, R., Legendre, P., Minchin, P., et al. (2022). vegan community ecology package version 2.6–2 April 2022. Available at: <http://CRAN.R-project.org/package=vegan>
- Okuda, K. (2002). Structure and phylogeny of cell coverings. *J. Plant Res.* 115, 283–288. doi: 10.1007/s10265-002-0034-x
- Orellana, L. H., Francis, T. B., Ferraro, M., Hehemann, J.-H., Fuchs, B. M., and Amann, R. I. (2022). Verrucomicrobiota are specialist consumers of sulfated methyl pentoses during diatom blooms. *ISME J.* 16, 630–641. doi: 10.1038/s41396-021-01105-7
- Orsi, W. D., Richards, T. A., and Francis, W. R. (2018). Predicted microbial secretomes and their target substrates in marine sediment. *Nat. Microbiol.* 3, 32–37. doi: 10.1038/s41564-017-0047-9
- Painter, T. J. (1983). “4 - algal polysaccharides” in *The polysaccharides*. ed. G. O. Aspinall (New York: Academic Press), 195–285.
- Pakulski, J. D., and Benner, R. (1994). Abundance and distribution of carbohydrates in the ocean. *Limnol. Oceanogr.* 39, 930–940. doi: 10.4319/lo.1994.39.4.0930
- Parks, D. H., and Beiko, R. G. (2015). “STAMP: statistical analysis of metagenomic profiles” in *Encyclopedia of metagenomics: Genes, genomes and metagenomes: Basics, methods, databases and tools*. ed. K. E. Nelson (Boston, MA: Springer US), 641–645.
- Parsons, T. R., Takahashi, M., and Hargrave, B. (1984). *Biological oceanographic processes*. Oxford Oxfordshire; New York: Pergamon Press.
- Passow, U. (2002). Transparent exopolymer particles (TEP) in aquatic environments. *Prog. Oceanogr.* 55, 287–333. doi: 10.1016/S0079-6611(02)00138-6
- Pedler, B. E., Aluwihare, L. I., and Azam, F. (2014). Single bacterial strain capable of significant contribution to carbon cycling in the surface ocean. *Proc. Natl. Acad. Sci. U. S. A.* 111, 7202–7207. doi: 10.1073/pnas.1401887111
- Peterson, A., Soberón, J., Pearson, R., Anderson, R., Martínez-Meyer, E., Nakamura, M., et al. (2011). *Ecological niches and geographic distributions* Princeton, NJ: Princeton University Press.
- Prahl, F. G., Sparrow, M. A., Eversmeyer, B., Ertel, J. R., and Goni, M. A. (1994). Terrestrial organic carbon contributions to sediments on the Washington margin. *Geochim. Cosmochim. Acta.* 58, 3035–3048. doi: 10.1016/0016-7037(94)90177-5
- Reintjes, G., Arnosti, C., Fuchs, B., and Amann, R. (2019). Selfish, sharing and scavenging bacteria in the Atlantic Ocean: a biogeographical study of bacterial substrate utilisation. *ISME J.* 13, 1119–1132. doi: 10.1038/s41396-018-0326-3
- Reintjes, G., Fuchs, B. M., Scharfe, M., Wiltshire, K. H., Amann, R., and Arnosti, C. (2020). Short-term changes in polysaccharide utilization mechanisms of marine bacterioplankton during a spring phytoplankton bloom. *Environ. Microbiol.* 22, 1884–1900. doi: 10.1111/1462-2920.14971
- Saier, M. H., Reddy, V. S., Moreno-Hagelsieb, G., Hendargo, K. J., Zhang, Y. C., Iddamsetty, V., et al. (2021). The transporter classification database (TCDB): 2021 update. *Nucleic Acids Res.* 49, D461–D467. doi: 10.1093/nar/gkaa1004
- Santillan, E., and Wuertz, S. (2022). Microbiome assembly predictably shapes diversity across a range of disturbance frequencies in experimental microcosms. *NPJ Biofilms Microbiomes* 8:41. doi: 10.1038/s41522-022-00301-3
- Sauer, D. B., Karpowich, N. K., Song, J. M., and Wang, D. N. (2015). Rapid bioinformatic identification of thermostabilizing mutations. *Biophys. J.* 109, 1420–1428. doi: 10.1016/j.bpj.2015.07.026
- Shi, Z., Xu, J., Li, X. F., Li, R. H., and Li, Q. (2019). Links of extracellular enzyme activities, microbial metabolism, and community composition in the river-impacted coastal waters. *J. Geophys. Res. Biogeosci.* 124, 3507–3520. doi: 10.1029/2019JG005095
- Sichert, A., Corzett, C. H., Schechter, M. S., Unfried, F., Markert, S., Becher, D., et al. (2020). Verrucomicrobia use hundreds of enzymes to digest the algal polysaccharide fucoidan. *Nat. Microbiol.* 5, 1026–1039. doi: 10.1038/s41564-020-0720-2
- Smith, M. W., Herfort, L., Rivers, A. R., and Simon, H. M. (2019). Genomic signatures for sedimentary microbial utilization of phytoplankton detritus in a fast-flowing estuary. *Front. Microbiol.* 10:2475. doi: 10.3389/fmicb.2019.02475
- Smits, S. A., Leach, J., Sonnenburg, E. D., Gonzalez, C. G., Lichtman, J. S., Reid, G., et al. (2017). Seasonal cycling in the gut microbiome of the Hadza hunter-gatherers of Tanzania. *Science* 357:802. doi: 10.1126/science.aan4834
- Sperling, M., Piontek, J., Engel, A., Wiltshire, K. H., Niggemann, J., Gerdt, G., et al. (2017). Combined carbohydrates support rich communities of particle-associated marine bacterioplankton. *Front. Microbiol.* 8:65. doi: 10.3389/fmicb.2017.00065
- Sun, J., Steindler, L., Thrash, J. C., Halsey, K. H., Smith, D. P., Carter, A. E., et al. (2011). One carbon metabolism in SAR11 pelagic marine Bacteria. *PLoS One* 6:e23973. doi: 10.1371/journal.pone.0023973
- Sun, C. C., Wang, Y. S., Li, Q. P., Yue, W. Z., Wang, Y. T., Sun, F. L., et al. (2012). Distribution characteristics of transparent exopolymer particles in the Pearl River estuary, China. *J. Geophys. Res. Biogeosci.* 117:G00N17. doi: 10.1029/2012JG001951
- Sun, C. C., Yue, W. Z., Wang, Y. S., He, W. H., Hong, Y. G., Sun, F. L., et al. (2022). Distribution of Coomassie blue stainable particles in the Pearl River Estuary, China, insight into the nitrogen cycling in estuarine system. *Front. Mar. Sci.* 8:73240. doi: 10.3389/fmars.2021.733240
- Teeling, H., Fuchs, B. M., Becher, D., Klockow, C., Gardebrecht, A., Bennis, C. M., et al. (2012). Substrate-controlled succession of marine bacterioplankton populations induced by a phytoplankton bloom. *Science* 336, 608–611. doi: 10.1126/science.1218344
- Teeling, H., Fuchs, B. M., Bennis, C. M., Kruger, K., Chafee, M., Kappelmann, L., et al. (2016). Recurring patterns in bacterioplankton dynamics during coastal spring algae blooms. *elife* 5:e11888. doi: 10.7554/eLife.11888
- Teufel, F., Armenteros, J. J. A., Johansen, A. R., Gislason, M. H., Pihl, S. I., Tsigiris, K. D., et al. (2022). SignalP 6.0 predicts all five types of signal peptides using protein language models. *Nat. Biotechnol.* 40:1023. doi: 10.1038/s41587-021-01156-3
- Thomas, F., Le Duff, N., Wu, T. D., Chron, A., Uroz, S., Riera, P., et al. (2021). Isotopic tracing reveals single-cell assimilation of a macroalgal polysaccharide by a few marine Flavobacteria and Gammaproteobacteria. *ISME J.* 15, 3062–3075. doi: 10.1038/s41396-021-00987-x
- Tremblay, L., and Benner, R. (2006). Microbial contributions to N-immobilization and organic matter preservation in decaying plant detritus. *Geochim. Cosmochim. Acta* 70, 133–146. doi: 10.1016/j.gca.2005.08.024
- Tripp, H. J., Kitner, J. B., Schwabach, M. S., Dacey, J. W. H., Wilhelm, L. J., and Giovannoni, S. J. (2008). SAR11 marine bacteria require exogenous reduced Sulphur for growth. *Nature* 452, 741–744. doi: 10.1038/nature06776

- Vidal-Melgosa, S., Sichert, A., Ben Francis, T., Bartosik, D., Niggemann, J., Wichels, A., et al. (2021). Diatom fucan polysaccharide precipitates carbon during algal blooms. *Nat. Commun.* 12:1150. doi: 10.1038/s41467-021-21009-6
- Vollmer, W., Joris, B., Charlier, P., and Foster, S. (2008). Bacterial peptidoglycan (murein) hydrolases. *FEMS Microbiol. Rev.* 32, 259–286. doi: 10.1111/j.1574-6976.2007.00099.x
- Von Meijenfheldt, F. A. B., Hogeweg, P., and Dutilh, B. E. (2023). A social niche breadth score reveals niche range strategies of generalists and specialists. *Nat. Ecol. Evolut.* 7, 768–781. doi: 10.1038/s41559-023-02027-7
- Wang, Y. M., Pan, J., Yang, J., Zhou, Z. C., Pan, Y. P., and Li, M. (2020). Patterns and processes of free-living and particle-associated bacterioplankton and archaeoplankton communities in a subtropical river-bay system in South China. *Limnol. Oceanogr.* 65, S161–S179. doi: 10.1002/lno.11314
- Wegner, C. E., Richter-Heitmann, T., Klindworth, A., Klockow, C., Richter, M., Achstetter, T., et al. (2013). Expression of sulfatases in *Rhodopirellula baltica* and the diversity of sulfatases in the genus *Rhodopirellula*. *Mar. Genomics* 9, 51–61. doi: 10.1016/j.margen.2012.12.001
- Wolter, L. A., Mitulla, M., Kalem, J., Daniel, R., Simon, M., and Wietz, M. (2021). CAZymes in *Maribacter dokdonensis* 62-1 from the patagonian shelf: genomics and physiology compared to related flavobacteria and a co-occurring alteromonas strain. *Front. Microbiol.* 12:628055. doi: 10.3389/fmicb.2021.628055
- Xing, P., Hahnke, R. L., Unfried, F., Markert, S., Huang, S. X., Barbeyron, T., et al. (2015). Niches of two polysaccharide-degrading *Polaribacter* isolates from the North Sea during a spring diatom bloom. *ISME J.* 9, 1410–1422. doi: 10.1038/ismej.2014.225
- Zhang, J., and Ma, K. (2013). *Spaa: an R package for computing species association and niche overlap*.
- Zhang, Y.-L., and Ran, Y. (2014). Stable carbon and nitrogen isotopic, amino acids and lignin compositions and geochemical significance of particulate organic matter from the middle and lower reaches of the Pearl River. *Geochimica* 43, 114–121. doi: 10.19700/j.0379-1726.2014.02.002
- Zhang, Y., Xiao, W., and Jiao, N. Z. (2016). Linking biochemical properties of particles to particle-attached and free-living bacterial community structure along the particle density gradient from freshwater to open ocean. *J. Geophys. Res. Biogeosci.* 121, 2261–2274. doi: 10.1002/2016JG003390
- Zhang, H., Yohe, T., Huang, L., Entwistle, S., Wu, P. Z., Yang, Z. L., et al. (2018). dbCAN2: a meta server for automated carbohydrate-active enzyme annotation. *Nucleic Acids Res.* 46, W95–W101. doi: 10.1093/nar/gky418
- Zhao, Z. H., Baltar, F., and Herndl, G. J. (2020). Linking extracellular enzymes to phylogeny indicates a predominantly particle-associated lifestyle of deep-sea prokaryotes. *Sci. Adv.* 6:eaz4354. doi: 10.1126/sciadv.aaz4354